




## Article

# The Degradation Product of Ramipril Is Potentially Carcinogenic, Genotoxic and Mutagenic

Katarzyna Regulska <sup>1,\*</sup>, Agnieszka Matera-Witkiewicz <sup>2</sup>, Aleksandra Mikołajczyk <sup>2</sup> and Beata J. Stanisiz <sup>3,\*</sup><sup>1</sup> Greater Poland Cancer Center, 15th Garbary Street, 61-866 Poznań, Poland<sup>2</sup> Screening of Biological Activity Assays and Collection of Biological Material Laboratory, Wrocław Medical University Biobank, Faculty of Pharmacy, Wrocław Medical University, Borowska 211 A, 50-556 Wrocław, Poland<sup>3</sup> Chair and Department of Pharmaceutical Chemistry, Poznań University of Medical Sciences, 6th Grunwaldzka Street, 60-780 Poznań, Poland

\* Correspondence: katarzyna.regulska@wco.pl (K.R.); bstanisz@ump.edu.pl (B.J.S.)

**Abstract:** (1) Background: The aim of this study was to identify the degradation product of ramipril (RAM) formed under dry air and to verify its potential modes of carcinogenicity. We intended to check whether its formation and presence in final dosage forms could pose a cancer risk to humans who are treated with RAM due to cardiological indications. The carcinogenicity of this compound was evaluated with respect to two mechanisms: a potential direct DNA-damage and indirect toxicity, secondary to forming mutagenic N-nitroso metabolites. (2) Methods: Firstly, a forced ageing test under dry air was conducted for pure RAM in order to induce its degradation. The validated HPLC system was used to describe the kinetic order of this reaction. The emerging degradation impurity was identified by HPLC-MS. In the second stage, the cancer risk of the identified RAM degradant was predicted using a structure-based assessment by in silico QSAR model, employing three endpoints: carcinogenicity, genotoxicity and mutagenicity. In the third stage, the obtained QSAR results were experimentally verified. To verify genotoxicity prediction, in vitro micronucleus assay was employed. It enabled us to assess the potential direct DNA-damaging properties of RAM degradant at high concentrations (as screening series) and at concentrations usually observed in human blood (to mimic the clinical scenario). To verify the QSAR mutagenicity prediction, an in vitro Ames test was carried out. It was designed so as to detect two mechanisms of mutagenicity: a direct one (for pure degradant) and an indirect one (via N-nitroso-metabolites formation). N-nitroso-metabolites for mutagenicity assessment were obtained using NAP test. (3) Results: The kinetic mechanism of RAM degradation was first-order, the degradation rate constant was  $k = 1.396 \pm 0.133 \times 10^{-5} \text{ s}^{-1}$  ( $T = 373 \text{ K}$ ), thus the formation of impurity was rapid. Energy of activation was  $174.12 \pm 46.2 \text{ kJ/mol}$ , entropy was positive, thus reaction was bimolecular and favored; enthalpy was  $171.65 \pm 48.7 \text{ kJ/mol}$ , thus reaction was endothermic. Only one degradation impurity was formed, and it was identified as RAM diketopiperazine derivative (DKP). QSAR simulation predicted that DKP could be carcinogenic and genotoxic, but this result had only moderate reliability. DKP was also predicted to be non-mutagenic and this prediction was strong (endpoint score 0.2). The confirmatory micronucleus experiment for genotoxicity prediction suggested that DKP was cytotoxic and it could be also aneugenic at a high concentration (0.22 mg/mL), evidenced by a three-fold increase in micronuclei relative to the control (11.86:33.33%,  $p = 0.0184$ ). At physiologic concentrations, its cytotoxicity and genotoxicity did not occur. This means that the genotoxicity of DKP was limited by a threshold mechanism. In the mutagenicity in vitro assessment, pure DKP was not mutagenic, but its nitrosation product induced base substitutions mutations in test bacteria TA100 following metabolic activation at a concentration of 4.5 mg/mL, confirming its mutagenicity. (4) Conclusions: RAM rapidly cyclizes to diketopiperazine derivative under dry air. This impurity resides in drugs administered to patients. DKP is potentially aneugenic and cytotoxic at high concentrations, yet at concentrations typically occurring in human blood, this effect is unlikely. The exposure of patients to high concentrations of DKP, exceeding the typical blood level and standard RAM dosing, could lead to cancer development, thus the safe threshold for human exposure to DKP must be verified in follow-up in vivo experiments.



**Citation:** Regulska, K.; Matera-Witkiewicz, A.; Mikołajczyk, A.; Stanisiz, B.J. The Degradation Product of Ramipril Is Potentially Carcinogenic, Genotoxic and Mutagenic. *Appl. Sci.* **2023**, *13*, 2358. <https://doi.org/10.3390/app13042358>

Academic Editors: Beatriz Giner Parache and Laura Lomba Eras

Received: 5 January 2023

Revised: 4 February 2023

Accepted: 9 February 2023

Published: 12 February 2023



**Copyright:** © 2023 by the authors. Licensee MDPI, Basel, Switzerland. This article is an open access article distributed under the terms and conditions of the Creative Commons Attribution (CC BY) license (<https://creativecommons.org/licenses/by/4.0/>).

Based on our results, it is impossible to establish the maximum safe dose of pure DKP to humans. Furthermore, DKP itself is not mutagenic, but it is liable to the formation of mutagenic nitroso-metabolites *in vivo*. Nitroso-derivatives of DKP are *in vitro* mutagens and their real-life impact on humans must be further evaluated in *in vivo* studies. Until this is carried out, RAM should not be formulated by manufacturers using dry procedures to minimize DKP formation and reduce risk of human carcinogenesis, since DKP could cause cancer via two independent mechanisms: direct genotoxicity when the exposure over standard RAM dosing occurs, and indirect mutagenicity via *in vivo* N-nitrosamine formation.

**Keywords:** genotoxicity; N-nitroso compound; degradation; impurity; stability; diketopiperazine; QSAR

## 1. Introduction

Human exposure to external chemical carcinogens is a well-defined cancer risk factor that accounts for about 40% of malignancies worldwide [1]. Chemical carcinogens also include pharmaceuticals and their impurities, as per the International Agency for Research on Cancer Monographs; thus, for occupational and consumer safety protection, screening for drug carcinogenicity is internationally mandated by legal requirements. In the European Union, they are defined by the ICH S2 (R1) (“Genotoxicity testing and data interpretation for pharmaceuticals intended for human use”) [2] and ICH M3 (R2) (“Non-clinical safety studies for the conduct of human clinical trials for pharmaceuticals”) guidelines [3] pertaining to drug products as well as by the most recent ICH M7 (R1) (“Assessment and control of DNA reactive (mutagenic) impurities in pharmaceuticals to limit potential carcinogenic risk”) guideline [4] dealing with drug mutagenic impurities. These regulations remain effective for new drug substances and new drug products during their clinical development, and subsequent applications for marketing, and only in a few circumstances for post-approval submissions of marketed products. Notably, the ICH M7 (R1) guideline was not implemented until 2014. Hence, a considerable number of pharmaceuticals have remained outside its scope, based on their well-established use, leaving their potential carcinogenic impurities unverified. The accidental discovery of mutagenic N-nitrosodimethylamine impurity in well-established valsartan and ranitidine-containing products, followed by their global recall in 2018, ultimately uncovered the insufficiency of the existing procedures, prompting an immediate scientific and institutional response [5]. As a consequence, worldwide risk assessment and mutagenic impurity profiling of old pharmaceuticals has led to the withdrawal of over 1800 batches of various finished formulations, until now, including sartans, antidiabetics, antihistamines and antibiotics in the United States, only due to mutagenic contaminants [6]. Even recently, in March 2022, all batches of propranolol extended-release capsules were recalled in Canada for their contamination with mutagenic N-nitroso-propranolol [7]. This clearly illustrates the huge scale of drug carcinogenic impurities problem, warranting the need for constant safety monitoring. The postulate applies in particular to all pharmaceuticals indicated for chronic use, whose lifetime cumulative doses are the highest.

Mutagenic N-nitroso compounds, besides being potential drug impurities, can also be endogenously formed from N-nitrosable drug precursors treated with nitrite in the strongly acidic environment of gastric juice. Possible sources of nitroso metabolites are amine, amide, cyanamide, guanidine, hydroxylamine, amidine, hydrazine, hydrazide, piperazine and diketopiperazine structures, which are present in a large portion of drugs, making them theoretically nitrosable [6,8]. Drug-nitrite interaction products can easily form DNA adducts, either in the nucleus or in the mitochondria, via electrophilic interactions, which translates into their multidirectional carcinogenic potency [6]. Indeed, in a recent animal models study, reactive nitrosamines caused mutations in both nuclear and mitochondrial DNA, leading to upregulation of the beta-2-adrenergic-receptors-cholinergic-receptor-

nicotinic- $\alpha$ -7-subunit-dependent nitrosamine canonical signaling, resulting in lung tumor growth. This was mediated by a malfunction of mitochondrial-reactive oxygen species [9]. Nitrosamines also caused aberrations in the mitochondrial electron transport chain, subunits I, II and IV, consequently affecting transmembrane electric potential and increasing oxidative stress, as an alternative cancerogenic mechanism [10]. Additionally, nitrosamines can reversibly inhibit gap junction intercellular communication leading to cancer, recently confirmed by Tschernig [11]. Therefore, the World Health Organization experts board developed “Nitrosation Assay Procedure” (NAP test) to screen for the liability of pharmaceuticals to endogenous nitrosation. The conditions of the NAP test involve a fourfold excess of nitrite in an acidic solution which mimics *in vivo* nitrosation in the stomach. Unfortunately, this procedure has never been included in registration dossiers. Hence, the potential for endogenous nitrosation of pharmaceuticals remains unknown unless verified by scientific research [6]. It is therefore evident that the area of carcinogenic drug impurities and metabolites safety profiling still remains insufficiently supported by experimental data, which obviously poses a safety concern and explains the need for relevant toxicological studies, mainly for well-established pharmaceuticals of key clinical relevance and widespread use.

Ramipril (RAM) is a dicarboxylate-containing angiotensin-converting enzyme inhibitor (ACE-I) of major clinical importance due to its indications for long-term treatment of severe cardiovascular conditions [12,13]. It was patented in 1981 and approved in 1989 [14]. Its impurity assessment was not required by the ICH M7 (R1) guideline during the post-approval period, and therefore it is hardly to be expected from the industry. In 2019, its total number of prescriptions in the United States was nearly 4 million, while the estimated number of treated individuals was 854,000, indicating its broad patient exposure and significant impact on public health [15]. Concurrently, there has been a fair number of epidemiological studies demonstrating clear associations between ACE-Is (including RAM) and the development of malignancy, such as multiple myeloma, breast and lung cancer [16–22]. Furthermore, in lung cancer, high cumulative ACE-Is doses were associated with modestly increased odds of disease, while lower doses only showed neutral associations. The mechanism behind these effects has never been elucidated [20]. Based on the above-discussed insufficiency of safety profiling procedures in the group of well-established pharmaceuticals, a possible interpretation of these observations could be the carcinogenic impact of drug degradation impurities or N-nitroso metabolites, which have evaded the regulatory safety screening prior to drug approval, as was the case with valsartan and ranitidine. Such cause-effect relationships would be, however, hard to observe in the setting of observational case-control studies due to distant endpoints and multiple distracting factors. Therefore, the suggested correlation between RAM stability and its oncological safety must be verified by means of experimental methods.

According to our previous report, RAM is chemically unstable as its degradation is rapid, and within the pharmacological class of ACE-Is it is the most vulnerable to temperature and humidity changes. Its degradation impurities formed under humid conditions include: biologically-active ramiprilat and a diketopiperazine derivative (DKP) [15]. The available stability data for RAM are, however, incomplete. Its mechanism of degradation under dry air still remains unknown. Probably, the only degradation impurity formed under such conditions is DKP, as with other structurally-related ACE-Is [23,24]. This degradation pathway, in turn, is highly unfavorable from the clinical point of view, since DKP is pharmacologically inactive against RAM biological targets, its presence is of no clinical benefit and its toxicity to humans is unknown [15]. DKP also contains a diketopiperazine structural alert that is potentially susceptible to N-nitrosation *in vivo*, with further mutagenic hazard to patients, as discussed above [8]. Thus, we hypothesized that DKP formation in RAM dosage forms could be a possible reason for the reported increased cancer incidence, associated with ACE-I use. To verify this, we decided to perform this multistage study correlating the stability and safety features of RAM.

Taking all the above into consideration, the aim of our research was to check whether: (1) the degradation of RAM under dry air leads to the formation of DKP impurity; (2) RAM degradation impurity formed under dry air exerts a direct carcinogenic, genotoxic or mutagenic effect; (3) RAM degradation impurity formed under dry air exerts an indirect mutagenic effect by the formation of N-nitroso compounds *in vivo*. Our research plan was: (1) the detailed description of the kinetic mechanism of RAM degradation under dry air by appropriate qualitative and quantitative parameters; (2) the identification of the emerging degradation products; (3) a structure-based assessment of the identified impurity's cancer risk by *in silico* QSAR model, employing three endpoints: carcinogenicity, genotoxicity and mutagenicity; (4) the verification of the QSAR simulation for genotoxicity by *in vitro* micronucleus assay; (5) the verification of the QSAR simulation for mutagenicity by Ames test; (6) the verification of the vulnerability of the investigated impurity to form mutagenic N-nitroso metabolites by NAP test and subsequent Ames test.

Our intention was to check various potential mechanisms of carcinogenicity, involving direct genotoxicity, direct mutagenicity or indirect mutagenicity by forming mutagenic N-nitroso metabolites. We designed our studies so as to mimic *in vivo* conditions and reflect the environment of human body. Accordingly, we assumed that genotoxic agents act via threshold mechanisms. Thus, for direct genotoxicity assessment, by *in vitro* micronucleus assay, we employed two experimental series of a studied compound: a screening series at high concentrations to detect the exact mechanism of genotoxicity with high sensitivity, and the series with typical blood concentrations to check the real-life impact of RAM degradant after standard dosing. On the other hand, for mutagenicity assessment by Ames test, we assumed that mutagens, unlike genotoxic agents, act via direct modification of DNA nucleotide sequence at any concentration, so there is no safe level of exposure to such substances. For this reason, for the evaluation of mutagenic activity of RAM degradant and its nitroso-metabolite, only one series at high concentrations was involved, which increased the sensitivity of our assay [4].

## 2. Materials and Methods

### 2.1. Kinetic Studies

Pure RAM (100%) was purchased from Rolabo (Zaragoza, Spain, batch n<sup>o</sup>: 11.PT24.01.02). HPLC-grade methanol, acetonitrile, formaldehyde and potassium dihydrogen phosphate were purchased from Merck, Darmstadt, Germany.

Samples of RAM were weighted on analytical scale Satorius BP 2105. They were heated in thermal chambers WAMED KBC-125 W with automatic temperature and RH control (Wamed, Warsaw, Poland).

The kinetic analysis was performed using a Shimadzu liquid chromatograph (Shimadzu Corporation, Kyoto, Japan) consisting of a Rheodyne 7125, 100  $\mu$ L fixed loop injector, a UV-VIS SPO-6AV detector, an LC-6A pump and a C-RGA chromatopac integrator. The following operating conditions were applied: mobile phase consisting of acetonitrile–aqueous phosphate buffer, pH 2.0; 0.035 mol/L (65:35 *v/v*) and stationary phase consisting of LiChrospher 100 RP-18 (size 5  $\mu$ m) 250 mm  $\times$  4 mm I.D column. The chromatographic separation was isocratically performed at ambient temperature at a flow rate of 1.2 mL/min with the detector wavelength set at 215 nm. The injection volume was 20  $\mu$ L. The mobile phase had been filtered through a filter (0.22  $\mu$ m) and degassed by ultrasound prior to use.

The employed HPLC method was revalidated in order to confirm its applicability for the assessment of the RAM stability profile under dry air conditions. The following validation parameters were determined: selectivity, linearity, sensitivity, precision and accuracy according to procedures described in our previous publication [15]. They were in agreement with ICH guideline Validation of analytical procedures: Text and methodology Q2 (R1) [25]. For that purpose, a calibration curve was constructed; limit of detection (DL), limit of quantification (QL), coefficient of variation (CV) and recovery were calculated. The procedures for revalidation are provided in the Supplementary Material (Supplement S1: HPLC validation procedures).

The kinetic evaluation of RAM degradation was then conducted under stress conditions of elevated temperature, ranging from 353 K to 373 K and dry air (RH 0%). Samples of pure RAM (0.010 g) were analytically weighed into glass vials, placed into a sand bath and heated for different time intervals so as to induce degradation. Then, respective samples were dissolved in methanol to a total volume of 25.0 mL and filtered. The chromatograms were achieved. Basing on the chromatographic peaks areas, the contents of RAM and its degradation product were calculated (c) from the calibration curve. These results were plotted versus time (t) so as to construct kinetic curves:  $c = f(t)$  and kinetic equations. The kinetic model of the degradation was established by fitting the experimental data to the following theoretical equations: nucleation (power-law, Avrami-Erofeev, Prout-Tompkins), geometrical contraction (contracting area, contracting volume), diffusion (1D diffusion, 2D diffusion, 3D diffusion) and reaction-order (zero-order, first-order, second-order and third-order). The best fit, defined by the highest correlation coefficient, was identified. The degradation rate constants (k) were then calculated using least square method. Furthermore, thermodynamic parameters were evaluated based on the procedure described in our previous publication [15]. The relevant equations for the kinetic study procedures and thermodynamic calculations [26] are provided in Supplement S2: Thermodynamic parameters calculation.

### 2.2. Identification of RAM Degradation Product

To confirm the identity of the emerging degradation product, a sample of fully degraded RAM under the following experimental conditions:  $t = 90$  h; 373 K; RH 0%, was used. The product of RAM degradation was identified using a Liquid Chromatography/Electrospray Ionization-Mass Spectrometry System HPLC-MS (Waters ZQ with photodiode array detector (Waters 996 ZQ, Waters Corporation, Milford, MA, USA). LC separations were made on Hypersil MOS column, 5  $\mu\text{m}$  particle size, 250 mm  $\times$  4 mm at 35  $^{\circ}\text{C}$  (308 K). The mobile phase consisted of methanol-water-formaldehyde (49:50:1  $v/v/v$ ). Its flow rate was 0.5 mL/min. The mobile phase was filtered through a 0.22  $\mu\text{m}$  filter and degassed by ultrasound. The injection volume was 100  $\mu\text{L}$ . The recorded mass range was from  $m/z$  100 to 1000. Soft ionization technique—electrospray (ESI) was applied and the mass spectrometer was run in a negative (ES $^{-}$ ) and positive (ES $^{+}$ ) ionization mode. The spectral range was 200–400 nm. A molecular ion was identified. Its mass-to-charge ratio ( $m/z$ ) was compared to the molecular mass of the predicted degradation impurity in order to confirm its identity.

### 2.3. In Silico Prediction of Genotoxicity, Mutagenicity and Carcinogenicity

The kinetic study was followed by an in silico safety evaluation of the identified RAM degradation impurity in order to set the scope of further toxicological research in vitro. An open access software VEGA-GUI version 1.2.0 from [www.vegahub.eu](http://www.vegahub.eu) (accessed on 4 January 2023) was used for carcinogenicity, mutagenicity and genotoxicity prediction. The structure of the IMD derivative (a structural analogue of RAM) was tested in parallel in order to make a comparative analysis.

The employed VEGA platform accessed QSAR models, which correlated its internal dataset of structurally-related chemicals with target molecules. In the version 1.2.0, it has four models for mutagenicity, ten models for carcinogenicity, one model for chromosomal aberration and two for micronucleus activity. The models available for the mutagenicity endpoint (ISS, SARpy, CAESAR, Mutagenicity Read-Across/KNN) were built based on experimental data derived from in vitro studies (e.g., the Ames Test in *Salmonella typhimurium* strains), while the carcinogenicity models (ISS, ISSCAN-CGX, CAESAR, ANTARES) used data from in vivo studies in different species, mainly mice and rats. All the VEGA models differ in their analytical approach (rule-based expert system, correlation between relevant fragments with toxicological endpoint, regression models, hybrid models), all of which had been validated prior to their commercialisation and none of which was considered

inferior [27]. Thus, in this study, all of them were used to increase the predictive power of the stimulation.

The identifiers of the tested molecules in SMILES format were inserted into the task list of the analysis tool. Then, the QSAR models for toxicity endpoints were selected and the prediction reports for each model were computed. The VEGA output was exported in .pdf file with 'yes' or 'no' prediction relative to each endpoint. The results were supported by the information on the reliability of prediction, measured by VEGA by the use of an in-built applicability domain evaluation tool. It was expressed as the Applicability Domain Index (ADI), which was computed to compare the tested molecules with the model training set. For  $ADI > 0.85$ , the prediction was considered strong. For  $ADI < 0.65$ , the prediction was considered weak. The values in between were considered as moderate. This parameter was automatically analyzed by VEGA and it was integrated into a final wording result expressed as "low reliability", "moderate reliability", "good reliability" [27]. To compare the results obtained for different QSAR models, the scoring approach developed by Glück et al. [28] was employed. It translated VEGA wording results into numeric values (endpoint scores, ES) ranging from 0 to 1 where "1" represents high toxicity and "0" is low toxicity with respect to model endpoint. Then, the average  $ES_{av}$  was calculated and expressed as the arithmetical mean of the ES values for respective endpoints. To interpret these data, the cut-off values were adopted as follows:  $ES_{av} > 0.66$  for true-toxicity claim;  $ES_{av} < 0.33$  for true non-toxicity claim. Scores between 0.33 and 0.66 were considered as inconclusive.

#### 2.4. Micronucleus Assay Procedure

The degradation impurity of RAM was then subjected to in vitro micronucleus assay based on the results of the computed in silico simulations. To that end, DMEM (Dulbecco's Modified Eagle's Medium), FBS (Fetal Bovine Serum), L-glutamine, amphotericin B, penicillin-streptomycin, Aroclor 1254-induced male Sprague Dawley rat liver S9, mitomycin C, cyclophosphamide, colchicine and cytochalasin B were used. They were purchased from Sigma-Aldrich (St. Louis, MO, USA). HCS CellMask™ Green Stain and Hoechst 33342 were supplied by Thermo Fisher Scientific (Waltham, MA, USA).

L929 cell line (ECACC 85011425, mouse C3H/An connective tissue) was cultured in DMEM supplemented with 10% heat-inactivated FBS, 2 mM L-glutamine, 2.5 µg/mL amphotericin B, 100 U/mL penicillin and 100 µg/mL streptomycin. Cells were maintained at 37 °C (310 K) and 5% CO<sub>2</sub> in a humidified atmosphere. Cell cultures were passaged before they reached 90% confluency to maintain exponential growth. They were regularly checked for mycoplasma contamination. For the cytokinesis-block in micronucleus assay 24 h before treatment, cells were seeded into 6-well plates at a density of  $2.2 \times 10^5$  cells/well and incubated at 37 °C (310 K), 5% CO<sub>2</sub> in a humidified atmosphere. After the incubation time, cells were treated with tested compounds in the same 6-well plates.

The in vitro micronucleus test was performed in accordance with the guideline 487: In Vitro Mammalian Cell Micronucleus Test, from the Organization for Economic Co-operation and Development (OECD, 2016) [29]. In this study, two experimental series were carried out. The first one comprised three concentrations tested in duplicate: 2, 0.67, 0.22 mg/mL, for screening purposes. The concentrations and the number of replicates were selected basing on the recommendations of guideline 487 from OECD. In this setting, for each concentration, three experimental conditions were applied: short treatment with metabolic activation (6 h) and both, short (6 h) and long treatments (30 h) without metabolic activation, to investigate potential clastogenic and aneugenic activity. Metabolic activation was applied to detect genotoxic agents formed secondary to modifications by liver cytochromes. Hence, for each condition, different medium was required. For short treatment with metabolic activation, a culture medium with a 2% S9 mix to achieve metabolic activation was used. For short treatment without metabolic activation, only culture medium was necessary. For long treatment, medium with 2 µg/mL cytochalasin B as a cytokinesis inhibitor was applied.

In the second experimental series, three physiological concentrations of the tested compound were investigated. This experiment was designed in order to mimic a clinical

scenario and check the activity of RAM degradation impurity after the administration of a standard RAM dose to a patient. The concentrations were the following: 1, 10 and 100 nM (which correspond to:  $3.98 \times 10^{-7}$  mg/mL,  $3.98 \times 10^{-6}$  mg/mL,  $3.98 \times 10^{-5}$  mg/mL). They reflected blood levels of DKP, measured in blood samples derived from healthy individuals which were subjected to pharmacokinetic study [30]. Only the extended treatment conditions (30 h of treatment in the culture medium with cytochalasin B) without metabolic activation were applied, relying on the results obtained in the screening series.

Stock solutions were prepared in DMSO, and appropriate solvent vehicle controls were also contained in the assay. The concentration of DMSO did not exceed 1% of the final culture volume. Additionally, positive controls were used, including: mitomycin C (0.25 µg/mL), cyclophosphamide (0.25 µM) and colchicine (0.025 µg/mL), depending on the type of exposure. The type and the concentration of the controls were selected based on the recommendations of the OECD guideline 487 [29]. For cells with short treatment, after 6 h of incubation, medium was gently aspirated, cells were washed with PBS (Phosphate-Buffered Saline) and medium with 2 µg/mL cytochalasin B was added. Following 24-h incubation, cells were fixed with a 1:1 ethanol-methanol mix 2 mL per well. Fixed cells were co-stained with HCS CellMask™ Green Stain (300 µL per well, conc. 2 µg/mL) and Hoechst 33342 (300 µL per well, conc. 5 µg/mL) according to the manufacturer's protocol to reveal nuclei, micronuclei and surrounding cytoplasm. At least 500 cells were scored per one experimental condition. Among them, 100 binucleated cells were counted (if possible). The proportion of mono, bi- and multinucleated cells was also obtained to calculate the replication index (RI) and cytokinesis-block proliferation index (CBPI) to evaluate potential cytotoxicity, according to the formula below.

$$RI = \frac{((\text{No. binucleate cells}) + (2 \times \text{No. multinucleate cells})) / (\text{Total number of cells})_T}{((\text{No. binucleate cells}) + (2 \times \text{No. Multinucleate cells})) / (\text{Total number of cells})_C} \times 100$$

where T = treated and C = control.

$$CBPI = \frac{((\text{No. mononucleate cells}) + (2 \times \text{No. binucleate cells}) + (3 \times \text{No. multinucleate cells}))}{(\text{Total number of cells})}$$

where T = treated and C = control.

Then, the percentage of micronuclei found in binucleated cells relative to the control was established (% MN/BC). Concurrent negative controls (solvents only) were used for each experimental setting as indicators for the background frequency of micronuclei. Positive controls were used to demonstrate the ability to induce micronuclei formation. The percentage of induced micronuclei was assessed for binucleated cells.

### 2.5. NAP-Test Procedure

To verify the suspected indirect mutagenic activity of RAM degradation impurity, its potential to form mutagenic N-nitroso compounds in vivo was investigated using the NAP test.

Pepsin [n<sup>o</sup>: 9001-75-6] was bought from Pol-Aura, Poland. Analytical grade hydrochloric acid 1.0 mol/L, sodium nitrite (NaNO<sub>2</sub>) and ammonium sulfamate (NH<sub>4</sub>SO<sub>3</sub>NH<sub>2</sub>) were obtained from Merck, Darmstadt, Germany. Ultrapure water was used. Simulated gastric juice (SGJ) (pH 1.2) was prepared as per the Polish Pharmacopoeia (ed. XII, 2020) by dissolving 2 g of sodium chloride and 3.2 g of pepsin in 80 mL HCl (1 mol/L) and sufficient water to make 1000 mL [31].

The sample of RAM degradation product was dissolved in DMSO, adjusted to pH 1.2 using SGJ, and then treated with sodium nitrite (in a molar ration of 10:40 mM). Then, the pH was readjusted to 1.2. The obtained nitrosation mixture was incubated at a temperature of 37 °C (310 K) for 60 min in the dark on a shaker. The solvent with nitrite treatment was incubated under similar conditions as a negative control for the mutagenicity assay. The reaction was subsequently stopped by the addition of ammonium sulfamate (molar

ratio  $\text{NaNO}_2$  vs.  $\text{NH}_4\text{SO}_3\text{NO}_2$  was 4:4). The obtained reaction mixture was subjected to mutagenicity evaluation. The concentrations of the tested nitrosation product were expressed as concentrations of the parent compound prior to nitrosation, i.e., 4.5, 2.25, 1.125, 0.56, 0.28 mg/dL. This evidenced the level of degradation impurity exposure that may pose a safety concern.

#### 2.6. Mutagenicity Assay-Bacterial Reverse Mutation Test Procedure

Ames test was performed to verify the results of QSAR assessment for mutagenicity and to check the mutagenic activity of the N-nitroso metabolite of the tested compound. This procedure was chosen since it is the first choice option for mutagenicity assessment of pharmaceuticals according to the ICH M7 (R1) guideline. A commercial Ames MPF 98/100 microplate format mutagenicity assay kit (Xenometrix, Allschwil, Switzerland) with *Salmonella typhimurium* strains TA98 (containing frameshifts mutation hisD3052, rfa uvrB, pKM101) and TA100 (containing base-pair substitution mutation hisG46, rfa uvrB, pKM101) was used. It contained 2-nitrofluorene, 4-nitroquinolone-N-oxide (4-NQO), 2-aminoanthracene as positive controls, Aroclor 1254-induced rat liver fraction S9 as the activation system, sterile ampicillin (50 mg/mL), ready-to-use growth medium, exposure medium and indicator medium. For preparing the S9 mix, a ready-to-use kit from Xenometrix (Switzerland) containing Buffer Salts solution (phosphate buffer,  $\text{MgCl}_2$ , KCl, NADP solution, G-6-P solution) was employed. The tested samples were dissolved in sterile DMSO (Merck, Darmstadt, Germany).

A completely degraded RAM sample (RAM content ~0%) and the nitrosation mixture of the RAM degradation product ( $c = 112.6$  mg/mL) were subjected to mutagenicity analysis. The degradation product was dissolved in DMSO to obtain a concentration of 125.0 mg/mL. Then, the test procedure provided by Ames MPF Instruction for use was followed [32,33]. The *Salmonella typhimurium* strains TA98 and TA100 were grown overnight (15 h) in growth medium at 37 °C (310 K) on a shaker set at 250 rpm. The exposure concentrations were selected based on the pre-screening procedure for cytotoxicity and solubility using the TA98 strain, as per kit instructions [33]. The *Salmonella typhimurium* strains TA98 and TA100 were then exposed to the tested substances in the presence and absence of rat liver S9 fraction. In the experiments without a metabolic activation system, the following positive controls were used: 2-nitrofluorene (2.0 µg/mL) for TA98 and 4-nitroquinolone-N-oxide (0.1 µg/mL) for TA100. In the experiments with a metabolic activation system, 2-aminoanthracene was used as a positive control at a concentration of 1.0 µg/mL for TA98 and 2.5 µg/mL for TA100. For the experiment with the degradation product, the baseline concentration was 125.0 mg/mL. For the experiments with the nitrosation mixture, the baseline concentration of the parent compound was 112.6 mg/mL. A serial  $1/2$ -log dilution was performed on a 96-well plate. To that end, in the experiments without metabolic activation, the standard solutions were diluted with histidine-rich exposure medium. In the experiments with a metabolic activation system, the standard solutions were diluted with histidine-rich exposure medium and microsomal S9 fraction mix. Six stock concentrations were achieved. Approximately  $10^7$  bacteria for each strain were treated in triplicate with the following test concentrations: 5.0 mg/mL, 2.5 mg/mL, 1.25 mg/mL, 0.63 mg/mL, 0.31 mg/mL, 0.16 mg/mL for pure degradation product and 4.5 mg/mL, 2.25 mg/mL, 1.125 mg/mL, 0.56 mg/mL, 0.28 mg/mL, 0.14 mg/mL for the nitrosation mixture, in a 24-well plate. Treated bacteria were incubated at 37 °C (310 K) on a shaker (250 rpm) for 90 min. Then, pH indicator medium without histidine was used to dilute the exposure cultures. They were aliquoted into 48 wells of a 384-well plate (50 µL per well). This was followed by 48 h of incubation at 37 °C (310 K) to allow revertant bacteria to grow. The indicator medium contained a pH indicator dye, which changed colour from purple to yellow due to bacterial metabolism, if the mutation occurred. The scoring of positive wells (revertants) was visually performed. Mutagenicity was confirmed if at least a two-fold increase over the



baseline was observed ( $FIB > 2$ ). The baseline was defined as the mean number of positive wells in the negative controls plus one standard deviation (SD).

$$FIB = \text{mean number of positive wells} / \text{zero-dose baseline}$$
$$\text{Baseline} = \text{mean zero-dose control} + 1 \text{ SD}$$

For statistical analysis of the obtained results, the cumulative binominal test was applied and binominal B-value was calculated, as recommended by Xenometrix, Switzerland.

### 3. Results

#### 3.1. HPLC Re-Validation Report

The selectivity of the employed chromatographic system was confirmed. The obtained chromatograms had good peak resolution and quality (Figure 1). In the time range from 0 to 15 min, single, well-resolved, sharp and symmetrical peaks were found. No tailing or fronting appeared (Figure 1). Chromatogram A demonstrates a single peak at  $t_R \sim 7.5$  min obtained for the pure RAM sample. Chromatogram B was obtained for a sample of RAM exposed to degradation test conditions ( $t = 20$  h,  $T = 373$  K,  $RH 0\%$ ). It shows two completely separated peaks attributed to RAM  $t_R \sim 7.5$  min, and to the product of its degradation,  $t_R \sim 5.5$  min. Chromatogram C was obtained for a sample after full RAM degradation ( $t = 90$  h,  $373$  K). Here, the peak for RAM at  $t_R \sim 7.5$  min was not observed, meaning that the reaction was complete and no substrate (RAM) remained in the sample. The only peak in chromatogram C at  $t_R \sim 5.5$  min was attributed to a single RAM degradation product. No matrix background interferences were observed in any chromatogram. Therefore, the method was considered selective. It allowed to differentiate and quantify the studied molecules under the conditions of our experiment.

The linearity of the method was expressed by the regression parameters of the calibration curve, obtained by the analysis of the series of ten working stock solutions. The correlation coefficient was  $r = 0.998$ , slope was  $a \pm \Delta a = 142.3 \pm 6.44$ , intercept was  $b \pm \Delta b = 0.0471 \pm 0.15$ . The method was accurate, as recovery was from 99.33% to 100.13%, which was within the acceptable range of 90–110%. The precise-CV was from 0.86 to 1.01% (acceptance criterion  $CV < 2\%$ ), and sensitive (LOD was 0.0024% and LOQ was 0.0072%). The detailed validation report is provided in the Supplement S3: HPLC validation results. The method was accepted for further kinetic studies.

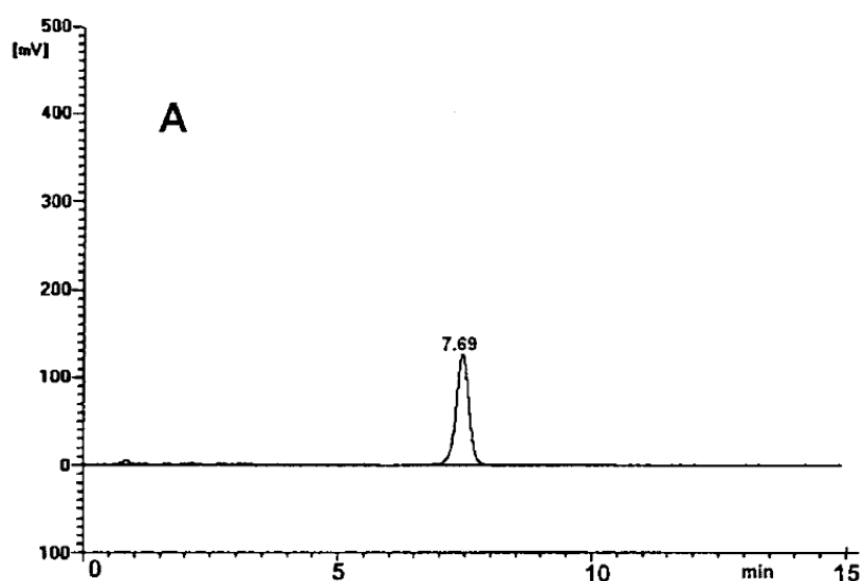
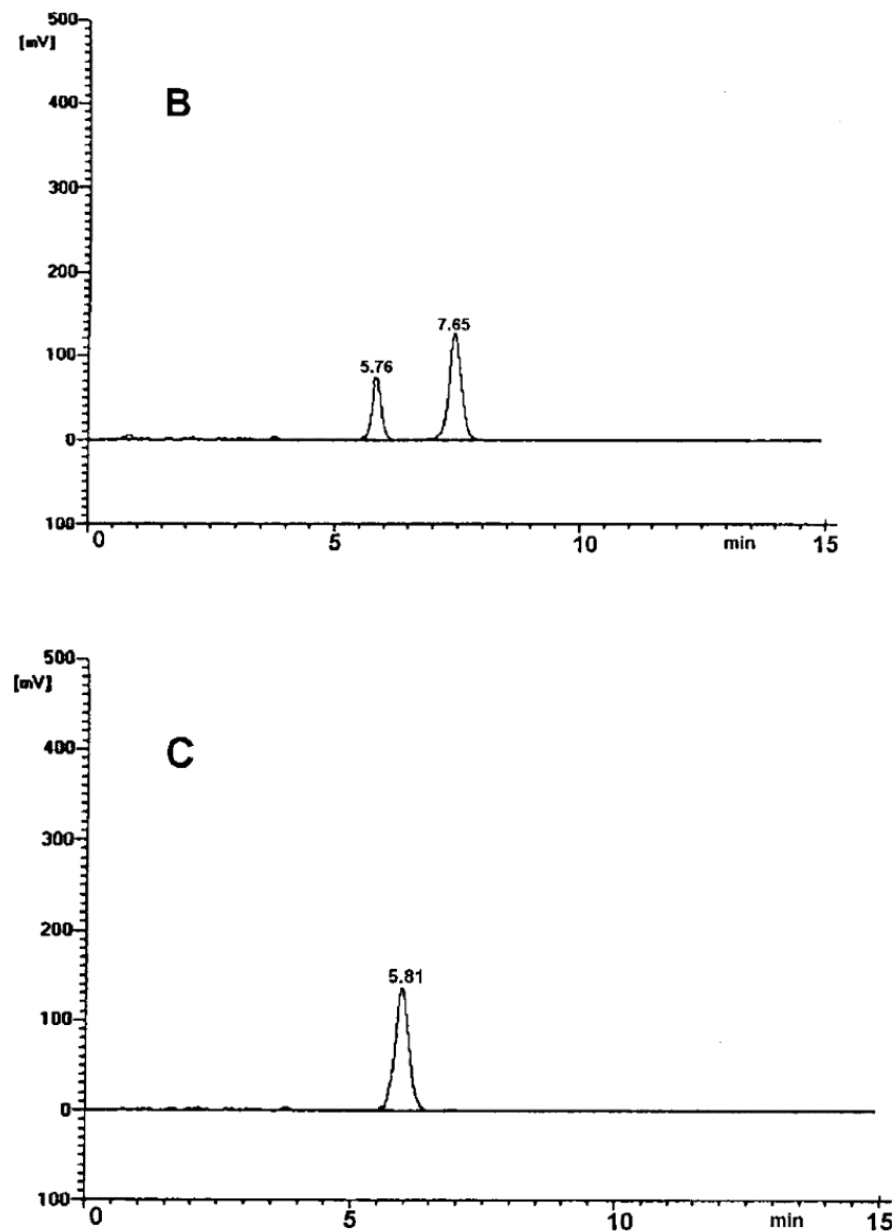


Figure 1. Cont.



**Figure 1.** HPLC chromatogram for: (A) undegraded RAM in solid state; (B) partially-degraded RAM ( $t = 20$  h, 373 K); (C) RAM after complete degradation ( $t = 90$  h, 373 K).

### 3.2. Kinetic Mechanism of RAM Degradation under RH 0%

The content of RAM in the stressed samples was established by the validated HPLC and plotted versus time of exposure. The content was expressed as the percentage of the remaining drug concentration, with 100% of RAM corresponding to  $t = 0$  h. The logarithmic kinetic curves were thus achieved (Figure 2). Then, they were transformed into semilogarithmic plots, and the straight lines were obtained for each sample series at each temperature, as depicted in Figure 2.

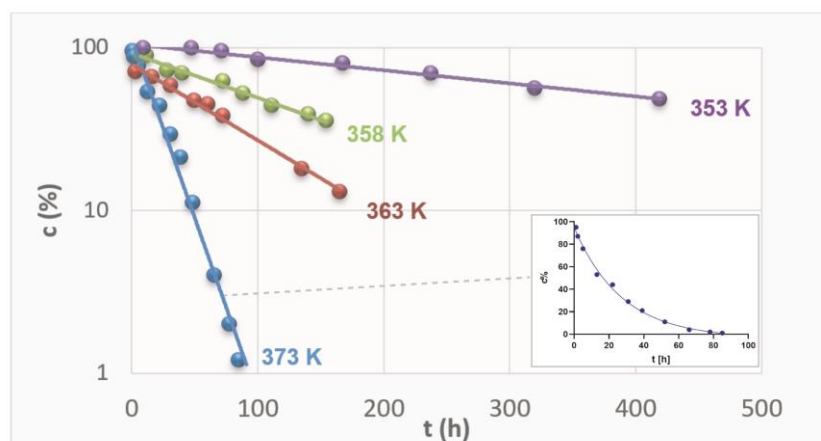


**Figure 2.** Semi-logarithmic plots  $c_t = f(t)$  describing degradation of RAM in solid state under dry air conditions at different temperatures.

Figure 2 demonstrates kinetic curves for RAM degradation at four different temperatures. It also demonstrates one logarithmic plot for a series at T 373 K as an example. For each experimental series, the gradual loss of RAM in stressed samples was confirmed. Furthermore, the higher the temperature, the more rapid the reaction was, as expressed by increasing slopes of the kinetic curves. The dots represent the contents of RAM ( $c\%$ ) in respective samples stressed under denotated temperatures for increasing time intervals. The most rapid loss of RAM was observed at the highest temperature tested ( $T = 373\text{ K}$ ), as the corresponding concentrations established by validated HPLC were the lowest. At lower temperatures, the decrease in RAM content in stressed samples was relatively less rapid. The F-test was performed for each linear regression and the obtained  $p$ -values confirmed that the correlations were significant and slopes were different from zero (Supplementary Material Table S2). Therefore, it was shown that the loss of RAM was proportional to time of exposure and its rate positively correlated with temperature level. Consequently, the reactions were found to follow first-order kinetics, irrespective of the temperature level, confirmed by the high correlation between the experimental data (Table 1). They were described by the following kinetic equation:

$$\ln c_t = \ln c_0 - k t$$

where  $c_t$  and  $c_0$  are concentrations of RAM in time  $t$  and 0, respectively,  $k$  is the first-order rate constant ( $s^{-1}$ ). The magnitude of  $k$  was then calculated as it corresponds to the slope of the obtained plot  $c = f(t)$  in the following manner:  $a = -k$  [26]. The kinetic and thermodynamic parameters of the reaction of RAM degradation were provided in Table 1. The corresponding raw data and their statistical analysis are provided in Supplement S4: Kinetic study results (Table S2).

**Table 1.** Kinetic and thermodynamic parameters of solid state RAM degradation under RH 0%.

T [K]	$k \pm \Delta k [s^{-1}]$	r	Linear Arrhenius Relationship $f(1/T) = \ln k_i$	Thermodynamic Parameters
353	$(5.340 \pm 0.395) \times 10^{-7}$	-0.997	$a = -20,943.07 \pm 5564.7$	$E_a [kJ/mol] = 174.12 \pm 46.2$
358	$(1.760 \pm 0.176) \times 10^{-6}$	-0.994	$s_a = 1748.81$	$\Delta H [kJ/mol] = 171.65 \pm 48.7$
363	$(3.289 \pm 0.431) \times 10^{-6}$	-0.992	$b = 45.03 \pm 15.4$	$\Delta S [J/mol \cdot K] = 0.12 \pm 12.5$
373	$(1.396 \pm 0.133) \times 10^{-5}$	-0.997	$s_b = 4.83$ $r = -0.993$ $F = 155.3$ $DFn, DFd = 1.2$ $p = 0.0064$	

Table 1 demonstrates the calculated degradation rate constants ( $k$ ) for RAM at four different temperatures. The provided  $k$  values are specific to the conditions at which they were obtained, and they describe the rate at which the reaction of RAM decay occurred. Their increasing magnitudes relative to temperature levels showed that RAM degradation accelerated with temperature, leading to drug content loss. In other words, the higher the temperature, the lower the RAM stability. The provided  $r$  values represent the correlation between experimental contents and time of stressing at each temperature level. Using  $t_{0.5} = 0.693/k$  formula, the half-life of RAM under dry air and  $T = 363$  K was calculated [15]. It equaled  $t_{0.5} = 5.8$  h, which means that, under the above conditions, after 5.8 h, the quantity of RAM would reduce to half of its initial amount. Interestingly, for humid conditions (RH 76%, and  $T = 363$  K) the half-life of RAM equaled 146 h [15], suggesting that under dry air RAM is less stable, and its degradation is more rapid. This observation was consistent with the corresponding  $k$  values: ( $k = (3.289 \pm 0.019) \times 10^{-6}$  for RH 0% vs.  $k = (1.343 \pm 0.093) \times 10^{-6}$  for RH 76%,  $T = 363$  [15]).

Table 1 also depicts the application of the Arrhenius equation to correlate the  $k$  values obtained for each temperature with the reciprocal of the corresponding temperature. In fact, Arrhenius regression is the most common mathematical model used for describing the relation between temperature and rate constant. The experimental degradation rate constants of RAM fulfilled the linear Arrhenius relationship  $\ln k = f(1/T)$  with good correlation ( $r = -0.993$ ), which further allowed the prediction of the thermodynamic behavior or RAM degradation under experimental conditions. The parameters of linear regression between experimental  $k$  values and respective temperatures, plotted according to Arrhenius equation, are provided in Table 1.  $S_a$  is the standard deviation of the intercept and  $S_b$  is the standard deviation of the slope. F-test confirmed that the correlation between  $\ln k$  and  $1/T$  is statistically significant in our experiment, as the slope of this plot was significantly different from zero ( $p = 0.0064$ ). This means that this equation can be used for data extrapolation and the prediction of  $k$  value (and RAM stability) at any temperature. Thermodynamic parameters were then predicted, including energy of activation ( $E_a$ ), enthalpy of activation ( $\Delta H$ ) and entropy of activation ( $\Delta S$ ), according to the transition state theory [26]. In our study, the observed reaction was endothermic as  $\Delta H$  was positive ( $\Delta H = 171.65 \pm 48.7$  kJ/mol), indicating that there was a need for a constant energy supply for the formation of the activated complex. Furthermore,  $\Delta S$  was positive ( $\Delta S = 0.12 \pm 12.5$  J/mol·K), thus the reaction was monomolecular and thermodynamically favored. On the contrary, for humid conditions  $\Delta S$  was negative and it equaled  $-92.01 \pm 189.2$  kJ/mol, suggesting that, in this case, the reaction was bimolecular. It must be also emphasized that the  $E_a$  for humid conditions was lower than that observed under dry air, and it equaled  $E_a = 96.39 \pm 22.4$  kJ/mol [15].

### 3.3. Identification of RAM Degradation Product

Based on the obtained MS spectra, the degradation impurity of RAM was verified. The relevant HPLC-ESI(+)-MS-TIC and HPLC-ESI(-)-MS-TIC chromatograms, recorded using three different scan modes, are provided in Figure 3. All of them show only one signal at  $t_R$  of about 7 min obtained for a completely degraded sample of RAM under the conditions of dry air ( $t = 90$  h,  $T = 373$  K). It meant that the tested sample contained only one compound, which was identified as RAM degradation impurity. The corresponding mass spectrum, provided in Figure 4, demonstrated one pseudomolecular ion at  $m/z = 399$  for ES+ and at  $m/z = 397$  for ES- (Figure 3). The value  $m/z$  stands for mass-to-charge ratio. As per electrospray ionization principle, the ES+ spectrum was obtained secondary to the attachment of one proton to the analyzed molecule, thus the mass of the resulting pseudomolecular ion was increased by the mass of proton  $[M + H]^+$  relative to the analyte (thus  $m_{\text{analyte}} = 399 - 1$ ); the charge of the molecule was +1. The ES- spectrum was, in turn, the result of molecule deprotonation  $[M - H]^-$ ; therefore, the mass of the pseudomolecular ion was actually reduced by the mass of proton relative to the analyte (thus,  $m_{\text{analyte}} = 397 + 1$ ); the charge of the molecule was -1. Consequently, the mass of the analyzed compound was established as  $m = 398$  u, as depicted in Table 2.

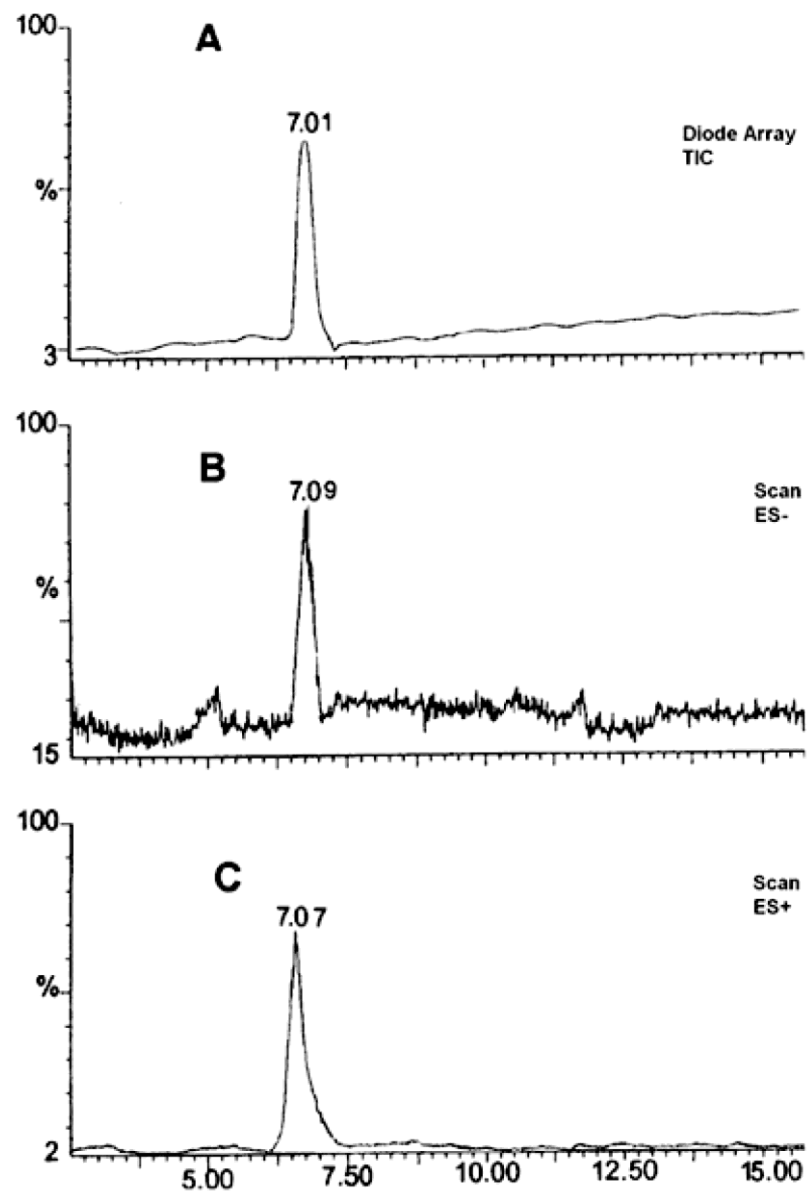


Figure 3. HPLC-ESI(+)-MS-TIC (A), HPLC-ESI(-)-MS-Scan (B), HPLC-ESI(+)-MS-Scan (C). Chromatogram for the analysis of RAM degradation impurity ( $t_R = 90$  h; 373 K) in solid state.

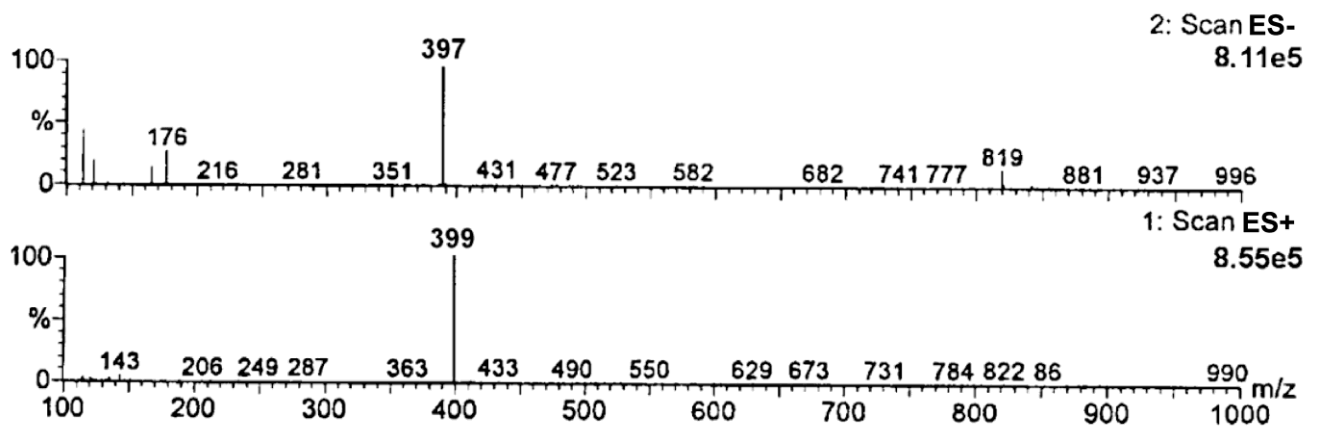


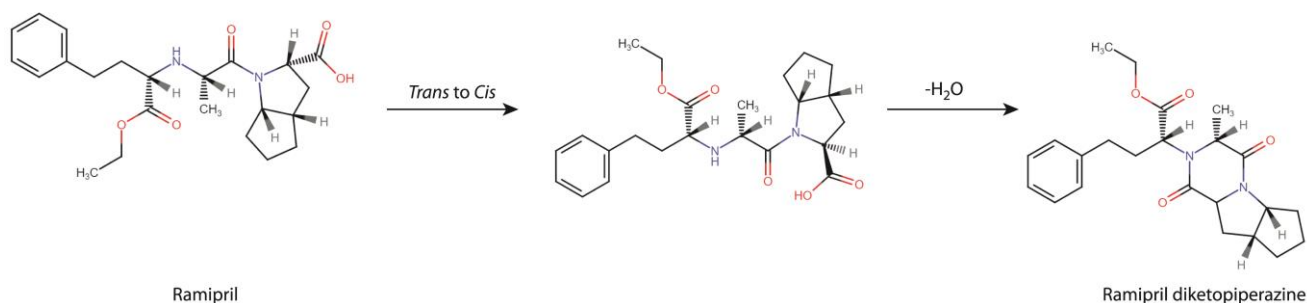
Figure 4. Mass spectra of RAM degradation impurity ( $t_R$  about 7 min).

**Table 2.** The  $m/z$  values of  $[M - H]^-$   $[M + H]^+$  for DKP and RAM.

Compound	Chemical Formula	Calculated Molecular Mass	Observed $m/z$ Value, ES <sup>-</sup> /ES <sup>+</sup>
Degradation impurity (DKP)	C <sub>23</sub> H <sub>30</sub> N <sub>2</sub> O <sub>4</sub>	398	399/397

The mass of the analyzed compound, established based on the obtained MS spectra, matched with the molecular mass of RAM intramolecular cyclization product—a dike-topiperazine derivative (DKP, chemical formula C<sub>23</sub>H<sub>30</sub>N<sub>2</sub>O<sub>4</sub>, molar mass M = 398 g/mol), as shown in Table 2.

It was finally concluded that the degradation of RAM under dry air conditions followed a single and rapid first-order reaction of intramolecular cyclization, producing a DKP derivative, as demonstrated in Figure 5. The reaction is in two stages. The first stage involves cis/trans transformation to adopt appropriate molecular conformation. Then, the escape of water molecules and the formation of new bonds occurs. A detailed discussion of the mechanism of DKP formation and its two-stage nature is provided in the Section 4.

**Figure 5.** RAM degradation pathway under dry air conditions.

### 3.4. QSAR Predictions for DKP Carcinogenicity

The identified degradation impurity was subsequently evaluated with respect to its cancer risk. The performed QSAR analysis provided predictions for DKP mutagenicity, genotoxicity and carcinogenicity using different *in silico* models, as reported in Table 3.

**Table 3.** QSAR predictions for DKP carcinogenicity, genotoxicity and mutagenicity.

VEGA Model	QSAR Prediction for DKP	Reliability ADI Index	Endpoint Scores (ES) [28]
Mutagenicity (Ames test) model (CAESAR) 2.1.13	NON-Mutagenic	High ADI = 0.948	0.1
Mutagenicity (Ames test) model (ISS) 1.0.3	NON-Mutagenic	Moderate ADI = 0.737	0.3
Mutagenicity (Ames test) model (SarPy-IRFMN) 1.0.8	NON-Mutagenic	High ADI = 0.948	0.1
Mutagenicity (Ames test) model (KNN-Read-Across) 1.0.1	NON-Mutagenic	Moderate ADI = 0.819	0.3
Carcinogenicity model (CAESAR) 2.1.10	Carcinogen	Low ADI = 0	0.5
Carcinogenicity model (ISS) 1.0.3	NON-Carcinogen	Moderate ADI = 0.749	0.3
Carcinogenicity model (IRFMN-ISSCAN-CGX) 1.0.1	Carcinogen; Structural alert for carcinogenicity defined by the SMARTS:CCCN(CC)CC	Moderate ADI = 0.67	0.7

Table 3. Cont.

VEGA Model	QSAR Prediction for DKP	Reliability ADI Index	Endpoint Scores (ES) [28]
Carcinogenicity model (IRFMN-Antares) 1.0.1	Carcinogen; Structural alert for carcinogenicity defined by the SMARTS: CCNCCCC(C)C	Low ADI = 0	0.5
Carcinogenicity oral classification model (IRFMN) 1.0.1	Carcinogen	Low ADI = 0	0.5
Carcinogenicity inhalation classification model (IRFMN) 1.0.1	NON-Carcinogen	Moderate ADI = 0.736	0.3
Chromosomal aberration model (CORAL) 1.0.1	Active–genotoxic	Moderate ADI = 0.617	0.7
In vitro Micronucleus activity (IRFMN-VERMEER) 1.0.1	Active–genotoxic Structural alert for micronucleus activity defined by the SMARTS: C(=O)NC(CO)C; O(CCN)C; C(O)C(C)N; C(CC)CCCC; CCCCCC; O=C(N)CCC; C(C(=O)O)NC; NC(C)C; C(=O)CCCC; NCCO; CCCCCCN; NCCNC; O=C(N)CC; CCCCC; CCC(C)C; C(C)(C)C; CN(CC)CC; C(C(=O))NC; N(C)(C)CCCCC; O=C(NCCO); C(C)CNCCO; O(C)CC(CC); O=C(N(C))CC	Low ADI = 0	0.5
In vivo Micronucleus activity (IRFMN) 1.0.2	Unable to predict		

The provided ADI value was used to measure the reliability of the prediction in a manner described in the Section 2. It corresponded with the wording result expressed as ‘low’, ‘moderate’ or ‘high’. Furthermore, the provided ES for each model were unified into average endpoint scores ( $ES_{av}$ ) for respective endpoints (mutagenicity, carcinogenicity, genotoxicity), calculated as an arithmetical mean. They were the following:  $ES_{av}$  for DKP non-mutagenicity equaled 0.2, for carcinogenicity models,  $ES_{av}$  was 0.5, while a combined  $ES_{av}$  for genotoxicity was 0.6.  $ES_{av}$  were used to make a final decision on respective endpoints’ reliability in a manner described in the Section 2. Unfortunately, the VEGA software was unable to predict the activity of DKP in in vivo micronucleus assays. In summary, DKP was predicted to be non-mutagenic with high reliability ( $ES_{av}$  0.2), carcinogenic with insufficient reliability ( $ES_{av}$  0.5) and genotoxic with insufficient reliability ( $ES_{av}$  0.6). Thus, the direct mutagenicity of DKP was excluded. The remaining results, although alarming, were not conclusive. For this reason, further toxicological assessment in an in vitro setting was conducted.

In addition to this, the same simulations were performed for a structural analog of DKP-IMD-DKP. These results are available in Supplement S5: QSAR predictions for IMD and IMD-DKP carcinogenicity, genotoxicity and mutagenicity. Here, the calculated  $ES_{av}$  for respective endpoints were the following: 0.15 for non-mutagenicity prediction, 0.3 for non-carcinogenicity and 0.5 for non-genotoxicity. The individual predictions for chromosomal aberration assay and in vivo micronucleus assay were negative, with moderate reliability. This suggests that IMD-DKP is neither mutagenic nor carcinogenic, while its genotoxic effect, despite the insufficient reliability of the model, is rather unlikely.

### 3.5. Micronucleus Assay

An in vitro micronucleus assay was carried out to verify the QSAR prediction for DKP genotoxicity. In this test, the cytotoxicity of the investigated compound was first evaluated, as it is a known confounding factor for micronuclei scoring. It was expressed as CBPI, RI and %cytotoxicity, as demonstrated in Table 4. The corresponding raw data for cell scoring are provided in Supplement S6: Micronucleus assay—cell scoring (Table S5).

**Table 4.** Cytostatic effect of DKP indicated by RI (Replication Index) and CBPI (Cytokinesis-Block Proliferation Index).

	Concentration	CBPI	RI	% Cytotoxicity	SD	% MN/BNC	<i>p</i> -Value One-Way ANOVA
Short treatment, −S9	DKP 2 mg/mL	1.00	0.00	100.00	±	0.0000	-
	DKP 0.67 mg/mL	1.15	23.35	76.65	±	7.5445	-
	DKP 0.22 mg/mL	1.79	125.71	−25.71	±	1.1930	0.4506
	mitC 0.25 µg/mL	1.23	35.88	64.12	±	0.5675	0.0070
	1% DMSO	1.63	100.00	-	-	-	8.28
Short treatment, +S9	DKP 2 mg/mL	1.00	0.29	99.71	±	0.4086	-
	DKP 0.67 mg/mL	1.08	11.12	88.88	±	3.6038	-
	DKP 0.22 mg/mL	1.64	89.39	10.61	±	4.2261	1.035
	CP 0.25 µM	1.16	22.05	77.95	±	2.4459	<0.0001
	1% DMSO	1.71	100.00	-	-	-	10.64
Extended treatment	DKP 2 mg/mL	1.01	1.70	98.30	±	0.1532	-
	DKP 0.67 mg/mL	1.01	0.83	99.17	±	0.3420	-
	DKP 0.22 mg/mL	1.12	16.85	83.15	±	1.3788	0.0184
	Col 0.025 µg/mL	2.27	181.55	−81.55	±	21.9522	0.0086
	1% DMSO	1.70	100.00	-	-	-	11.86
Extended treatment (physiological conc.)	DKP 100 nM	1.65	104.03	−4.03	±	3.5728	0.6404
	DKP 10 nM	1.65	104.23	−4.23	±	8.4285	0.9863
	DKP 1 nM	1.64	102.88	−2.88	±	2.5852	0.7308
	Col 0.025 µg/mL	1.82	132.03	−32.03	±	4.1326	<0.0001
	1% DMSO	1.62	100.00	-	-	-	9.16

The RI value represented the percentage of the number of cells that divided in the treated culture, compared to the number of cells that divided to form binucleate and multinucleate cells in the control culture, and it was used to calculate the % cytotoxicity. The CBPI indicated the average number of nuclei per cell. As depicted in Table 4, we found that, under the applied experimental conditions, DKP exerted a strong cytotoxic effect at high concentrations (screening series) in comparison with the control in all treatments (short S+, short S− and extended). Cytotoxicity was the most evident in extended treatment (99.71% and 90.30% for 0.67 mg/mL and 2 mg/mL, respectively). Since it exceeded  $55 \pm 5\%$  (defined by the OECD 487 guideline as a reliability criterion), cells treated with 0.67 and 2 mg/mL DKP were not included in determining the percentage of micronuclei among binucleated cells.

In screening series, in both short treatments, the induction of micronuclei at a concentration of 0.22 mg/mL was not observed, suggesting no clastogenic activity of DKP. However, in the extended treatment, the induction of micronuclei relative to the negative control was three-fold (11.86:33.33%,  $p = 0.0086$ ,  $\alpha = 0.05$ ), suggesting a statistically significant genotoxicity of DKP via aneugenic effect. However, this result cannot be considered as clearly positive because of potential disturbances from the high cytotoxicity of DKP. Therefore, additional tests, preferably in in vivo settings, are necessary to define the genotoxicity of DKP more conclusively.

The experiment was then repeated for extended treatment mode at physiological concentrations because, only for the extended treatment in the screening series, the genotoxic effect was observed. At micromolar concentrations, no cytotoxicity occurred and the number of micronuclei in binucleated cells was not increased when compared to the



negative controls ( $p > 0.05$ ,  $\alpha = 0.05$ ). Thus, genotoxicity was not observed. This means that, at physiological concentrations, the genotoxicity of DKP is unlikely.

### 3.6. Mutagenicity Assay

To verify the QSAR prediction for the carcinogenicity and mutagenicity of DKP, two potential mechanisms of mutagenicity were checked by in vitro Ames test. Therefore, two experimental series were performed. The first experiment with DKP aimed at the verification of direct DNA-reactivity of the studied compound. The experiment with DKP nitrosation mixture (N-DKP), in turn, was to check the potential indirect mechanism of DKP carcinogenicity, involving nitrosamine formation after the NAP test. The highest tested concentration of DKP was 5 mg/mL and of N-DKP—4.5 mg/mL. None of these concentrations were cytotoxic against the TA98 strain. The number of revertants in treated cultures was achieved, and the results of plate scoring are provided in Tables 5 and 6. The detailed data are demonstrated in Supplement S7: Mutagenicity assay results. FIB and B-value were adopted as criteria for determining mutagenicity. The primary criterion was FIB, and the supporting criterion was B-value.

**Table 5.** The results of bacterial reverse mutation test for DKP.

DKP c (mg/mL)	TA98 –S9		TA98 +S9		TA100 –S9		TA100 +S9	
	FIB	B-Value	FIB	B-Value	FIB	B-Value	FIB	B-Value
Baseline	12.03		4.72		4.87		5.32	
0.16	0.64	0.5854	0.42	0.4460	0.55	0.4069	0.69	0.9353
0.31	0.47	0.1160	0.35	0.2943	0.41	0.1691	0.56	0.8000
0.63	0.47	0.1160	0.28	0.1662	0.27	0.0399	0.31	0.2531
1.25	0.58	0.4043	0.21	0.0767	0.21	0.0144	0.19	0.0612
2.5	0.53	0.2382	0.42	0.4460	0.21	0.0144	0.63	0.8818
5	0.55	0.3172	0.99	0.9954	0.27	0.0399	0.13	0.0207
K+	3.97	1.0000	10.00	1.0000	8.43	1.0000	8.08	1.0000

K+—positive control, FIB—Fold increase over baseline, B-value—indicates the probability that spontaneous mutations events alone.

As shown in Table 5, for pure DKP, the number of revertants at each concentration was not relatively increased compared to the control in any experiment performed (details in Supplement S7: Mutagenicity assay results). The FIB value below 2 indicates that the difference between the mean number of revertants in the control and exposition was not statistically different. The binominal B value below 0.99 suggests that the probability of spontaneous mutations was 99%. This means that DKP did not induce point mutations in either TA98 or TA100 strains at any of the tested concentrations. Therefore, the direct mutagenic effect of DKP by frameshift mutations or base-pair substitution was ultimately excluded.

**Table 6.** The results of bacterial reverse mutation test for DKP nitrosation mixture (N-DKP).

N-DKP c (mg/mL)	TA98 –S9		TA98 +S9		TA100 –S9		TA100 +S9	
	FIB	B-Value	FIB	B-Value	FIB	B-Value	FIB	B-Value
Baseline	12.03		4.72		5.32		4.87	
0.14	0.91	0.9911	0.14	0.0270	0.65	0.6613	0.37	0.3892
0.28	0.94	0.9950	0.14	0.0270	0.53	0.4110	0.66	0.8961
0.56	0.80	0.9372	0.49	0.5987	0.53	0.4110	1.18	0.9998
1.125	0.94	0.9950	0.14	0.0270	0.95	0.9703	0.96	0.9953
2.25	0.78	0.9062	0.28	0.1662	0.36	0.1018	1.69	1.0000
4.5	0.80	0.9372	0.35	0.2943	0.47	0.2874	3.09	1.0000
K+	3.97	1.0000	10.00	1.0000	7.30	1.0000	9.49	1.0000

K+—positive control, FIB—Fold increase over baseline, B-value—indicates the probability that spontaneous mutations events alone.

For N-DKP (Table 6), the induction of revertants in the TA98 strain was not statistically different from the control (FIB was below 2). For concentrations of 0.14, 0.28 and

1.125 mg/mL, in the experiment without metabolic activation, the binomial B-value exceeded 0.99, which means that chances of spontaneous mutations were below 1% in these treatments. However, the primary criterion for mutagenicity was FIB; thus, these treatments were not considered mutagenic. In the experiment with TA100 without metabolic activation, FIB was also below 2 and B-value was below 0.99 for each concentration, so mutagenicity was not observed in this setting. However, for the TA100 strain with metabolic activation, N-DKP was mutagenic at the highest tested concentration (FIB was above 2 and B-value = 1). It can be, therefore, concluded that N-DKP induced a base-pair substitution mutation in *Salmonella typhimurium* TA100 strains following metabolic modification by mitochondrial enzymes; therefore, it was found to be a mutagen.

The results from Tables 5 and 6 are graphically demonstrated in Figure 6.

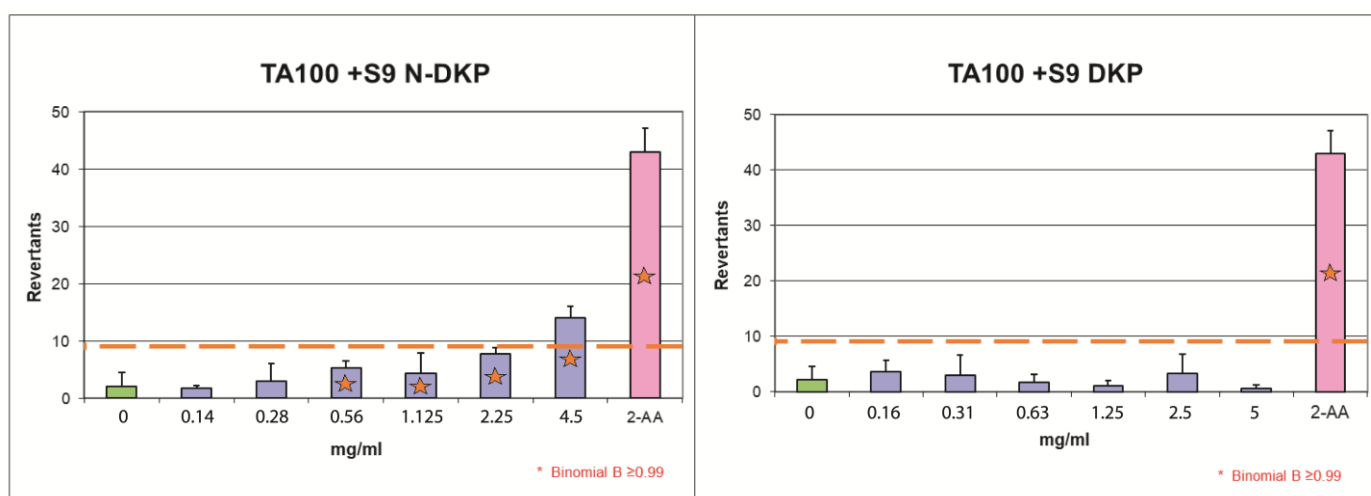


**Figure 6.** The results of bacterial reverse mutation test with TA100 strain with metabolic activation for the nitrosation mixture of DKP (N-DKP) and pure DKP.

Figure 6 graphically demonstrates the results of the Ames test for the experiments with DKP and N-DKP using the TA100 strain in the setting of metabolic activation. The raw data behind this graph are provided in Supplement S7: Mutagenicity assay results (Tables S11 and S13). The orange dashed line represents a two-fold increase over baseline, over which mutagenic activity was detected. The blue bars correspond to the mean number of revertants found in each concentration. The green bar represents the number of revertants scored for the negative control (solvent) and the pink bar is the positive control. Red asterisks indicate concentrations for which the B-value was above critical at 0.99. For concentrations marked with asterisks but below the dashed line, mutagenicity might be suspected; however, this prediction was not reliable as the criterion of FIB > 2 was the primary one. Only N-DKP, at a concentration of 4.5 mg/mL, following metabolic activation in the TA100 strain, provided a clear positive result for mutagenicity.

#### 4. Discussion

These studies were designed and performed as a follow-up to the existing reports that suggested a possible carcinogenic effect of ACE-Is on humans, caused by the unknown mechanism. In this context, we intended to verify whether these actions could have been associated with the formation of toxic degradation impurities in the dosage forms of RAM, routinely administered to patients. We considered so, because the correlation between ACE-Is stability and toxicity, despite the existing theoretical rationale, still remains unexplored. We selected RAM as a model molecule due to its widespread clinical use, poor stability profile and incomplete stability information. Hence, to fulfill our research plan, we had to supplement the lack of data on RAM degradation kinetics under dry air and to then perform a well-structured toxicological assessment.

The first step of our project aimed at providing a detailed description of RAM degradation behavior under the conditions of dry air, combined with the identification of the emerging degradation products. For that purpose, we developed and validated a HPLC stability-indicating protocol, which can now be also successfully applied for similar assays by manufacturers. Using this method, we managed to establish the kinetic parameters of RAM degradation under dry air and then to compare them with the corresponding ones, previously reported for RAM at humid conditions (RH 76%). Here, we found that, at RH 0%, the degradation of RAM follows first-order kinetics, meaning that its rate solely depends on the concentration of the parent compound. First-order reactions are preferred for drugs, due to their predictable and easy-to-control progress. On heating, the degradation accelerates, as evidenced by increasing  $k$  values with temperature, yet its kinetic order remains unaltered (Table 1). For RAM under humid conditions, similar observations have been previously made. However, with the lack of environmental moisture, the rate of RAM degradation and its thermodynamics changed, as well as its degradation products' yield when compared to RH 76%. In detail, at RH 0%, the reaction progressed more rapidly when compared to RH 76%, as shown by a higher degradation rate constant and shorter half-life. Simultaneously, the  $E_a$  of RAM degradation under dry air was increased relative to that reported for humid conditions. This means that, under dry air, the initiation of RAM degradation requires a higher energy input. Finally, the RAM degradation pathway was changed, as in the present study, it was found to follow a single intramolecular cyclization with the formation of DKP. On the contrary, the degradation of RAM in the presence of moisture involved two parallel reactions, i.e., hydrolysis and cyclization, with the former one being dominant. Hence, unlike dry air conditions, under humid conditions, the major degradation impurity was RAM diacid. The main reason for these variations between dry and humid environments is the obvious lack of water molecules to participate in hydrolytic bond cleavage in the environment of dry air. Thus, at RH 0%, intramolecular cyclization is the only possible degradation pathway. Under humid conditions, in turn, although cyclization actually occurs, it is very limited in scope. This is probably caused by the fact that it requires a higher  $E_a$  than hydrolysis. Hence, it is not favored. As a consequence, in the presence of moisture, DKP is only minimally formed, while under dry air its yield equals 100%, as shown in our experiments (Figure 1C). Furthermore, despite a high energy barrier between substrates and the activated complex under dry air (high  $E_a$ ), once initiated RAM cyclization proceeds very fast. Probably, this is caused by the two-stage nature of this process, as shown in Figure 5. Firstly, the adoption of an appropriate molecular conformation by RAM occurs. The second stage is deprotonation of the reacting amine, the addition of neutral nitrogen to the carbonyl of the neighboring carboxylic acid to form a tetrahedral intermediate, the escape of water molecules and a final new bond formation. Here, the rate-limiting step of this process is the *cis/trans* transformation of RAM, associated with multiple bond rotations and a consequent high energy consumption, defined by high  $E_a$  (Table 1,  $\Delta E_a = 174.12$  kJ/mol). The subsequent water loss is thermodynamically favorable (as supported by positive  $\Delta S$ , Table 1); hence, its rapid progression translates into a high value of the reaction rate constant. At RH 76%, no conformational changes are necessary for water molecules to access the ester bond in RAM; thus, the  $E_a$  for RAM hydrolysis under humid conditions is relatively low. Our findings are significant from a manufacturing point of view. Employing dry formulation methods would lead to compromised RAM stability, secondary to dry air degradation, which would be faster than that at humid conditions. Furthermore, the impurity profile would be affected, with DKP becoming a major degradant instead of RAM diacid. As a result, on heating and dry-processing, RAM would rapidly cyclize to DKP with all downstream consequences on its clinical and toxicological performance. Therefore, the application of dry procedures for RAM in the industry should be avoided.

In the next stage of this study, we decided to assess the impact of the RAM degradation mechanism on its safety. We only focused our interest on DKP since the toxicological data for both RAM and RAM diacid are available in the registration dossiers of commercially

available RAM dosage forms. Based on the literature background, which suggested a possible carcinogenic activity of ACE-Is, we performed a preliminary *in silico* QSAR simulation assessing various oncologic endpoints, i.e., the general carcinogenicity, mutagenicity and genotoxicity of DKP. Mutagenicity refers to the capacity of chemicals to cause changes in DNA sequences, leading to mutations, while genotoxicity causes damage to genomes, i.e., DNA or chromosomes. The genotoxic agents that cause structural chromosomal aberrations are clastogens, while those that cause numerical chromosomal aberrations are aneugens. The main practical difference between mutagenicity and genotoxicity is that mutagens have no threshold level and any exposure to them is hazardous. Thus, they are not allowed in final dosage forms. Genotoxic agents, in turn, act via threshold mechanisms and their low exposure is not always associated with cancer outcome. Thus, their safe concentration must be established and maintained in drug formulations. The results obtained from our QSAR simulations allowed us to classify DKP as a non-mutagen, as the calculated endpoint score ( $ES_{av} = 0.2$ ) fell within the non-mutagenicity criteria. The reliability of this prediction was high. Despite this, the adopted *in silico* model suggested other mechanisms of toxicity, i.e., the carcinogenic and genotoxic activity of DKP, but these predictions were not sufficiently reliable ( $ES_{av} = 0.5$  and  $0.6$ , respectively). On this basis, we assumed that DKP is a potential carcinogen that acts via a mechanism unrelated to direct DNA damage (non-mutagen), probably via chromosome damage (genotoxic agent). However, due to the insufficient reliability of the QSAR simulation for the genotoxicity endpoint, follow-up experiments were necessary, either by *in vitro* micronucleus or by chromosome aberration assay.

The *in vitro* mammalian cell micronucleus test for the genotoxicity assessment of DKP was selected as a follow-up to our QSAR simulations. The study was designed so as to screen for both aneugenic (aneuploidy-inducing) or clastogenic (chromosome-damaging) activity of the investigated compound. To that end, different treatment modes were applied (a short one for clastogens and an extended one for aneugens). Because genotoxic substances usually have a threshold mechanism, two experimental series of concentrations were conducted. The first series involved high concentrations of DKP, and it was employed to screen for the exact mechanism of genotoxicity. The second series covered physiological concentrations of DKP that corresponded to the level ordinarily present in the blood of patients treated with RAM due to cardiological indications. The second series enabled us to show the real-life activity of DKP after standard RAM dosing.

Firstly, the cytotoxicity of DKP was established, as this effect is a known confounding factor for micronuclei scoring. Notably, under the conditions of our test, the investigated degradation impurity exhibited a significant cytotoxic activity, exceeding 55.5%, as shown in Table 4, especially in the extended treatment setting in the screening series. Hence, only one screening concentration (0.22 mg/mL) was subjected to micronuclei scoring. For this concentration, in both short treatments, the percentage of micronuclei relative to the control was not increased, suggesting no clastogenic potential of DKP ( $p > 0.05$ , Table 4). On the contrary, based on the statistically significant, three-fold increase in micronuclei formation observed in the extended treatment mode, DKP was suggested to act as an aneugen ( $\% \text{ MN/BMN} = 33.33$ ,  $p = 0.0184$ ). This means that DKP could interact with proteins involved in the segregation of chromosomes during mitotic cell division, rather than DNA, leading to chromosome loss via micronuclei formation. Notably, it is typical for aneugenic substances that their effect only occurs in a narrow range of concentrations with a sublinear dose-response relationship; thus, their threshold dose can be estimated, as suggested by Lynch et al. [34]. As a consequence, low doses of aneugens induce zero effect, which was actually evidenced for DKP in our study, as shown in Table 4; at its physiological (micromolar) concentrations, the micronuclei were not formed ( $p < 0.05$ ). This means that standard dosing of RAM should not pose a carcinogenic risk in humans with respect to the suspected genotoxicity of DKP. However, the threshold level of DKP, above which the aneugenic effect is manifested, remains unknown. It falls between the tested series, and it should be established, preferably in follow-up *in vivo* studies; for example, using an *in vivo* micronucleus assay. This knowledge is necessary to set the safe level of

human exposure to this impurity. Furthermore, the observed significant cytotoxicity of DKP is also representative of a typical aneugen [34]. In fact, high doses of aneugens cause severe genomic imbalance and launch cell death mechanisms, leading to cell elimination, as was the case in our study. The high cytotoxic potency of DKP can be also explained by its structural features. Its changeable chiral and rigid skeleton favors its easier binding to molecular targets; for example, Aurora kinases or tubulin, both of which participate in chemical-induced aneugenicity in vitro [35]. Interestingly, this property of other DKP analogs, i.e., unsaturated 2,5-diketopiperazine derivatives, was examined in a number of human tumor cell lines, in which a 2,5-diketopiperazine ring was set as an optimal scaffold for exploring anticancer drug candidates [36]. Nonetheless, in the context of our studies, it must be emphasized that aneuploidy caused by aneugens is an important, but not independent, contributor to cancer development [37]. For this reason, a direct genotoxic/aneugenic activity of excessive doses of DKP combined with other carcinogenic factors is necessary to induce cancer in humans. Consequently, we further investigated other mechanisms of carcinogenicity of DKP; i.e., its mutagenic activity and the mutagenic activity of its N-nitroso metabolite. Obviously, our conclusions need confirmatory, in vivo experiments because the cytotoxicity of DKP could have disturbed the micronuclei scoring in our studies, while our QSAR model predicting DKP carcinogenicity/genotoxicity was not sufficiently reliable to provide unquestionable conclusions. In addition to this, no other DKP derivatives of ACE-Is had been subjected to in vitro micronucleus assay before, thus no comparative analysis was possible. Despite these limitations, we believe that the evidence from our investigations is sufficient to set follow-up in vivo experiments, without further confirmatory in vitro protocols [38]. Therefore, we strongly suggest that the aneugenicity threshold of DKP and its impact on living organisms should to be evaluated under in vivo conditions by marketing authorization holders in order to validate the acceptable limits of this impurity in formulated drugs.

Finally, due to the presence of a diketopiperazine structural alert in the RAM degradation product, potentially leading to the formation of mutagenic nitroso compounds, we performed mutagenicity evaluation for pure DKP and its nitrosation product using the Ames test. To that end, the NAP test was first carried out using SGJ, which served as an in vitro model of DKP nitrosation in the stomach. Then, pure DKP and the product of its nitrosation (N-DKP) were subjected to mutagenicity evaluation. Both compounds were tested only at high concentrations, since mutagens have no threshold mechanism and their exposure is hazardous at any level. High concentrations were therefore applied to increase the sensitivity of our assay. The obtained results (Table 5) showed that pure DKP was not mutagenic, which was consistent with our QSAR predictions. In other words, pure DKP is not reactive against DNA. On the other hand, for N-DKP, a mutagenic effect was observed in the *Salmonella typhimurium* T100 system, with S9 fraction at 4.5 mg/mL (FIB = 3.09; B = 1.00, Table 6). This indicates that DKP nitrosation products cause mutations by base substitutions upon activation by liver cytochromes. The possible products of DKP-nitrite interaction could involve the N-nitrosoramipril formed by the DKP ring opening or N-nitrosodiketopiperazine derivative, formed secondary to the loss of carboxyphenylalanine moiety. Our result corresponds with the reported mechanism of mutagenic action of N-nitrosamines. In fact, their emerging electrophilic metabolites, produced by cytochrome catalytic activity, easily alkylate nuclear DNA and thus, contribute to cancer initiation [39]. This justifies the fact that the mutagenic effect of N-DKP occurred in the experiment with metabolic activation. This also means that there is no safe level of N-DKP and its presence in human blood at any concentration could induce cancer. Given that the only source of N-DKP in humans is DKP formed secondary to RAM degradation, the content of this impurity in drug formulation must be minimized.

Based on our results, it can be therefore concluded that the carcinogenic effect of DKP in humans is probable and it may be manifested via two independent mechanisms: direct aneugenic activity at excessive doses as a secondary factor, and indirect mutagenic action secondary to in vivo transformation to nitroso-metabolites. Here, it must be also noted

that independent aneugenicity of pure DKP at standard blood levels is rather unlikely. The nitroso-metabolites of DKP, in turn, are mutagenic irrespective of blood level, and they could be the reason for increased cancer incidence among RAM users independently. The relevance of these in vitro findings must be verified in in vivo settings. Until this is done, one strategy to minimize the risk of human exposure to mutagenic DKP-nitrite metabolites might be employing additional stabilization methods by manufacturers so that DKP is not formed. Furthermore, antioxidants such as ascorbic acid or  $\alpha$ -tocopherol added to final RAM formulation could serve as a mitigation strategy to eliminate electrophilic nitroso-radicals endogenously formed from DKP. Antioxidants can also be introduced as a supportive therapy, for example, by using quercetin-loaded nanostructures lipid carriers, which were effective in preventing oxidative stress induced by paraquat in vitro [40].

At this point, it is also important to emphasize that our studies are pioneering in the field of genotoxicity, mutagenicity and nitrosation screening for drug impurities. In fact, the only similar report is available for IMD degradation impurities, and it was prepared well before the worldwide nitrosamine crisis by our research team [8,33]. Other toxicological studies regard either final drug products or active pharmaceutical ingredients. Drug degradation impurities, in turn, have been paid minimal attention until now, even though they are also present in drug formulations, and hence, their cancer risk needs evaluation as well. As evidenced recently by Schmidtsdorff et al. [6], nitrosamine metabolites are common among different groups of pharmaceuticals, since, in their study, a total of 33 out of 67 pro-drugs were found to produce nitrosamine derivatives using the NAP test. Furthermore, in the study by Ozahn et al. [41], 22 drugs (including enalapril) out of 28 examined formed mutagenic nitroso-compounds, verified with *Salmonella typhimurium* TA 1535/pSK1002 in vitro assay. We believe that screening for the nitrosation potential of drug degradation impurities would provide similar proportions.

A final remark on our project is that a structural analog of RAM-DKP, IMD-DKP was not mutagenic in the Ames test, neither in pure nor in nitrosation mixtures [8,33]. Hence, it can be stated that IMD-DKP remains non-reactive in the presence of nitrite, or else its nitrosation products induce no mutations. Furthermore, VEGA-GUI simulations assessing the oncological endpoints of IMD-DKP were favorable and reliable. Only the predictions for non-genotoxicity were insufficiently supported by an applicability domain of the corresponding models. However, since IMD-DKP is clearly non-carcinogenic, its genotoxicity is rather improbable. Furthermore, IMD-DKP is less likely to appear in final dosage forms, as IMD is more stable than RAM ( $t_{0.5 \text{ RH } 76.4\% \text{ T363K}} = 177 \text{ h}$  and  $t_{0.5 \text{ RH } 76.4\% \text{ T363K}} = 14 \text{ h}$ , respectively) [15,42], indicating its better safety profile. Therefore, we hypothesized that IMD should receive more clinical attention over RAM, especially in patients with high risk of cancer development.

Our study has several limitations. In fact, the employed in vitro and in silico systems are not fully representative of real-life conditions. In the process of drug research and development, they serve as screening procedures to provide rationale for further invasive studies. Therefore, our findings need confirmatory experiments in animal models for carcinogenicity. This postulate is extremely important, since RAM is a valuable cardiology drug, and for this reason it is crucial to both guarantee its safety and assess its benefit-to-risk ratio without any confounding factors.

## 5. Conclusions

In our study, we managed to describe the mechanism of RAM degradation under dry air. We proved that such conditions compromise RAM stability and promote its rapid degradation via intramolecular cyclization. The only degradant formed at RH0% was DKP. From QSAR simulations, we established that DKP was a potential carcinogen acting by a genotoxic mechanism. However, this prediction needed confirmatory studies due to its insufficient reliability. The QSAR model also suggested that DKP was a non-mutagen with high reliability. In in vitro studies, we found two potential mechanisms of DKP-induced carcinogenicity; i.e., the direct aneugenic action of excessive doses and

indirect mutagenicity secondary to the *in vivo* formation of N-nitroso metabolites. From the *in vitro* micronucleus assay, we found that DKP was a cytotoxic and aneugenic agent at high concentrations. At normal blood concentrations, DKP was neither cytotoxic nor aneugenic. Hence, due to the potential aneugenicity, the safe level of DKP must be evaluated in follow-up *in vivo* studies, as excessive doses above normal blood concentrations could contribute to cancer as a supporting factor. Our results do not establish a threshold concentration of DKP. Concurrently, no clastogenic effect is expected from DKP based on *in vitro* micronucleus assay. Furthermore, from the *in vitro* Ames test, DKP was not a direct mutagen. However, it can form nitroso derivatives *in vivo*, which induce base-pair substitution mutations upon metabolic activation in the liver. Nitroso-metabolites of DKP were mutagenic in the Ames test; thus, it was concluded that no safe level of DKP nitroso-metabolites exists. This can be extrapolated to DKP as it is the only source of DKP-nitroso derivatives *in vivo*. Consequently, it is probable that RAM dry air degradation could be associated with increased cancer incidence, secondary to forming reactive, mutagenic nitroso-metabolites and by inducing aneugenic damage of genomes at high concentrations. For this reason, dry formulation methods and excessive heating must be avoided in RAM technological processing. The real-life significance of our findings must be verified in follow-up *in vivo* experiments.

**Supplementary Materials:** The following supporting information can be downloaded at: <https://www.mdpi.com/article/10.3390/app13042358/s1>. Supplement S1: HPLC validation procedures. Supplement S2: Thermodynamic parameters calculation. Supplement S3: HPLC validation results. Supplement S4: Kinetic study results. Supplement S5: QSAR prediction for IMD and IMD-DKP carcinogenicity, genotoxicity and mutagenicity. Supplement S6: Micronucleus assay—cell scoring. Supplement S7: Mutagenicity assay results.

**Author Contributions:** K.R.: conceptualization; data curation; formal analysis; funding acquisition; investigation; methodology; project administration; resources; software; supervision; validation; visualization; original draft writing; review and editing, A.M.-W.: resources, formal analysis, draft writing, funding acquisition, supervision, A.M.: resources, investigation; formal analysis, draft writing, B.J.S.: supervision. All authors have read and agreed to the published version of the manuscript.

**Funding:** This research was funded by Greater Poland Cancer Center, grant No. 4/2020(235).

**Institutional Review Board Statement:** Not applicable.

**Informed Consent Statement:** Not applicable.

**Data Availability Statement:** The data presented in this study are available in DOI:10.3390/pharmaceutics13101600.

**Acknowledgments:** HPLC-MS analysis was performed in the Laboratory of faculty of Chemistry, A Mickiewicz University, Poznan, Poland. The procedure of Ames test was performed in Department of Toxicology, Poznan University of Medical Sciences, Poznan, Poland. *In vitro* micronucleus test was performed in Screening of Biological Activity Assays and Collection of Biological Material Laboratory, Wroclaw Medical University, Poland.

**Conflicts of Interest:** The authors declare no conflict of interest.

## References

1. Madia, F.; Worth, A.; Whelan, M.; Corvi, R. Carcinogenicity assessment: Addressing the challenges of cancer and chemicals in the environment. *Environ. Int.* **2019**, *128*, 417–429. [[CrossRef](#)] [[PubMed](#)]
2. European Medicines Agency. ICH S2 (R1) Genotoxicity Testing and Data Interpretation for Pharmaceuticals Intended for Human Use. Available online: <https://www.ema.europa.eu/en/ich-s2-r1-genotoxicity-testing-data-interpretation-pharmaceutics-intended-human-use-scientific> (accessed on 23 February 2020).
3. European Medicines Agency. ICH M3 (R2) Non-Clinical Safety Studies for the Conduct of Human Clinical Trials for Pharmaceuticals. Available online: <https://www.ema.europa.eu/en/ich-m3-r2-non-clinical-safety-studies-conduct-human-clinical-trials-pharmaceutics-scientific> (accessed on 23 February 2020).

4. European Medicines Agency. ICH M7 (R1) Assessment and Control of DNA Reactive (Mutagenic) Impurities in Pharmaceuticals to Limit Potential Carcinogenic Risk. Available online: [https://www.ema.europa.eu/en/documents/scientific-guideline/draft-ich-guideline-m7-assessment-control-dna-reactive-mutagenic-impurities-pharmaceuticals-limit\\_en.pdf](https://www.ema.europa.eu/en/documents/scientific-guideline/draft-ich-guideline-m7-assessment-control-dna-reactive-mutagenic-impurities-pharmaceuticals-limit_en.pdf) (accessed on 23 February 2020).
5. Regulska, K.; Michalak, M.; Murias, M.; Stanisz, B. Genotoxic impurities in pharmaceutical products—Regulatory, toxicological and pharmaceutical considerations. *J. Med. Sci.* **2021**, *90*, 116–120. [[CrossRef](#)]
6. Schmidtsdorff, S.; Neumann, J.; Schmidt, A.H.; Parr, A.K. Risk assessment for nitrosated pharmaceuticals: A future perspective in drug development. *Arch. Pharm.* **2022**, *355*, 2100435. [[CrossRef](#)]
7. Government of Canada, Recalls and Safety Alerts: Pfizer Recalls Inderal-LA (Propranolol Hydrochloride) Capsules Due to a Nitrosamine Impurity. Available online: <https://www.canada.ca> (accessed on 22 October 2022).
8. Regulska, K.; Murias, M.; Stanisz, B.; Regulski, M. The mutagenicity analysis of imidapril hydrochloride and its degradant, diketopiperazine derivative, nitrosation mixtures by in vitro Ames test with two strains of *Salmonella typhimurium*. *Rep. Pract. Oncol. Radiother.* **2014**, *19*, 412–419. [[CrossRef](#)]
9. Sarlak, S.; Lalou, C.; Sant’Anna-Silva, A.C.B.; Mafhouf, W.; De Luise, M.; Rousseau, B.; Izotte, J.; Claverol, S.; Lacombe, D.; Nikitopoulou, E.; et al. Lung Tumor Growth Promotion by Tobacco-Specific Nitrosamines Involves the  $\beta$ 2-Adrenergic Receptors-Dependent Stimulation of Mitochondrial REDOX Signaling. *Antioxid. Redox Signal.* **2022**, *36*, 525–549. [[CrossRef](#)] [[PubMed](#)]
10. Homšak, M.; Trampuž, M.; Naveršnik, K.; Kitanovski, Z.; Žnidarič, M.; Kiefer, M.; Časar, Z. Assessment of a Diverse Array of Nitrite Scavengers in Solution and Solid State: A Study of Inhibitory Effect on the Formation of Alkyl-Aryl and Dialkyl *N*-Nitrosamine Derivatives. *Processes* **2022**, *10*, 2428. [[CrossRef](#)]
11. Tschernig, T. Connexins and Gap Junctions in Cancer of the Urinary Tract. *Cancers* **2019**, *11*, 704. [[CrossRef](#)]
12. Regulski, M.; Regulska, K.; Stanisz, B.; Murias, M.; Gieremek, P.; Wzgarda, A.; Niznik, B. Chemistry and Pharmacology of Angiotensin-Converting Enzyme Inhibitors. *Curr. Pharm. Des.* **2015**, *21*, 1764–1775. [[CrossRef](#)]
13. The European Society of Cardiology and the European Society of Hypertension. 2018 ESC/ESH Guidelines for the management of arterial hypertension: The Task Force for the management of arterial hypertension of the European Society of Cardiology (ESC) and the European Society of Hypertension (ESH) 2018 ESC/ESH Clinical Practice Guidelines for the Management of Arterial Hypertension. *Eur. Heart J.* **2018**, *39*, 3021–3104. [[CrossRef](#)]
14. Fischer, J.; Ganellin, C.R. *Analogue-Based Drug Discovery*; John Wiley & Sons: Hoboken, NJ, USA, 2006; p. 469. ISBN 9783527607495.
15. Regulska, K.; Musiał, J.; Stanisz, B.J. Solid-State Stability Profiling of Ramipril to Optimize Its Quality Efficiency and Safety. *Pharmaceutics* **2021**, *13*, 1600. [[CrossRef](#)]
16. Regulska, K.; Regulski, M.; Karolak, B.; Michalak, M.; Murias, M.; Stanisz, B. Beyond the boundaries of cardiology: Still untapped anticancer properties of the cardiovascular system-related drugs. *Pharmacol. Res.* **2019**, *147*, 104326. [[CrossRef](#)] [[PubMed](#)]
17. Buchler, T.; Krejci, M.; Svobodnik, A.; Adam, Z.; Minarik, J.; Bacovsky, J.; Scudla, V.; Mayer, J.; Vorlicek, J.; Hajek, R. Outcome of patients with multiple myeloma and hypertension treated with angiotensin-I-converting enzyme inhibitors during high-dose chemotherapy. *Hematol. J.* **2005**, *5*, 559–564. [[CrossRef](#)] [[PubMed](#)]
18. Hicks, B.M.; Fillion, K.B.; Yin, H.; Sakr, L.; Udell, J.A.; Azoulay, L. Angiotensin converting enzyme inhibitors and risk of lung cancer: Population based cohort study. *BMJ* **2018**, *363*, k4209. [[CrossRef](#)] [[PubMed](#)]
19. Boudreau, D.M.; Yu, O.; Chubak, J.; Wirtz, H.S.; Bowles, E.J.A.; Fujii, M.; Buist, D.S.M. Comparative safety of cardiovascular medication use and breast cancer outcomes among women with early stage breast cancer. *Breast Cancer Res. Treat.* **2014**, *144*, 405–416. [[CrossRef](#)]
20. Kristensen, B.; Hicks, B.; Azoulay, L.; Pottgård, A. Use of ACE (Angiotensin-Converting Enzyme) Inhibitors and Risk of Lung Cancer: A Nationwide Nested Case-Control Study. *Circ. Cardiovasc. Qual. Outcomes* **2021**, *14*, e006687. [[CrossRef](#)]
21. Lin, S.-Y.; Lin, C.-L.; Lin, C.-C.; Hsu, W.-H.; Lin, C.-D.; Wang, I.-K.; Hsu, C.-Y.; Kao, C.-H. Association between angiotensin-converting enzyme inhibitors and lung cancer—a nationwide, population-based propensity score-matched cohort study. *Cancers* **2020**, *12*, 747. [[CrossRef](#)]
22. Meng, L.; Yang, B.; Qiu, F.; Jia, Y.; Sun, S.; Yang, J.Q.; Huang, J. Lung Cancer Adverse Events Reports for Angiotensin-Converting Enzyme Inhibitors: Data Mining of the FDA Adverse Event Reporting System Database. *Front. Med.* **2021**, *8*, 594043. [[CrossRef](#)]
23. Wzgarda, A.; Dettlaff, K.; Mostalska, M.; Pabian, E.; Regulska, K.; Stanisz, B.J. Thermo-, Radio- and Photostability of Perindopril Tert-butylamine in The Solid State. Comparison to Other Angiotensin Converting Enzyme Inhibitors. *Iran J. Pharm. Res.* **2017**, *16*, 1007–1018.
24. Regulska, K.; Stanisz, B.; Regulski, M.; Murias, M. How to design a potent, specific, and stable angiotensin-converting enzyme inhibitor. *Drug Discov. Today* **2014**, *19*, 1731–1743. [[CrossRef](#)]
25. European Medicines Agency. ICH Guideline Validation of Analytical Procedures: Text and Methodology Q2 (R1). Available online: <https://www.ema.europa.eu/en/ich-q2r2-validation-analytical-procedures-scientific-guideline> (accessed on 23 February 2020).
26. Bhangare, D.; Rajput, N.; Jadav, T.; Sahu, A.K.; Tekade, R.K.; Sengupta, P. Systematic strategies for degradation kinetic study of pharmaceuticals: An issue of utmost importance concerning current stability analysis practices. *JAST* **2022**, *13*, 7. [[CrossRef](#)]
27. Benfenati, E.; Manganaro, A.; Gini, G. VEGA-QSAR: AI Inside a Platform for Predictive Toxicology. In Proceedings of the workshop “Popularize Artificial Intelligence 2013”, Turin, Italy, 5 December 2013; CEUR Workshop Proceedings: Krasnoyarsk, Russia, 2013; Volume 1107.



28. Glück, J.; Buhrke, T.; Frenzel, F.; Braeuning, A.; Lampen, A. In silico genotoxicity and carcinogenicity prediction for food-relevant secondary plant metabolites. *Food Chem. Toxicol.* **2018**, *116 Pt B*, 298–306. [[CrossRef](#)]
29. Polish Pharmacopoeia XII. 4.1.1 Reagents, Standard and Buffer Solutions; Polish Pharmacopoeia: Warszawa, Poland, 2020; p. 719.
30. OECD. Test No. 487: In Vitro Mammalian Cell Micronucleus Test. In *OECD Guidelines for the Testing of Chemicals*; Section 4; OECD Publishing: Paris, France, 2016. Available online: <https://doi.org/10.1787/9789264264861-en> (accessed on 12 January 2021).
31. Levitt, D.G.; Schoemaker, R.C. Human physiologically based pharmacokinetic model for ACE inhibitors: Ramipril and ramiprilat. *BMC Clin. Pharmacol.* **2006**, *6*, 1. [[CrossRef](#)] [[PubMed](#)]
32. OECD. Test No. 471: Bacterial Reverse Mutation Test. In *OECD Guidelines for the Testing of Chemicals*; Section 4; OECD Publishing: Paris, France, 2020. Available online: <https://doi.org/10.1787/20745788> (accessed on 12 January 2021).
33. Regulska, K.; Murias, M.; Stanisz, B.; Regulski, M. Is there any association between imidapril hydrochloride stability profile under dry air conditions and cancer initiation? *Int. J. Pharm.* **2013**, *456*, 332–339. [[CrossRef](#)] [[PubMed](#)]
34. Lynch, A.M.; Eastmond, D.; Elhajouji, A.; Froetschl, R.; Kirsch-Volders, M.; Marchetti, F.; Masumura, K.; Pacchierotti, F.; Schuler, M.; Tweats, D. Targets and mechanisms of chemically induced aneuploidy. Part 1 of the Report of the 2017 IWGT workgroup on assessing the risk of aneuploidy for carcinogenesis and hereditary diseases. *Mut. Res.* **2019**, *847*, 403025. [[CrossRef](#)] [[PubMed](#)]
35. Wang, Y.; Wang, P.; Ma, H.; Zhu, W. Developments around the bioactive diketopiperazines: A patent review. *Expert Opin. Ther. Pat.* **2013**, *23*, 1415–1433. [[CrossRef](#)] [[PubMed](#)]
36. Liao, S.-R.; Qin, X.-C.; Wang, Z.; Li, D.; Xu, L.; Li, J.-S.; Tu, Z.-C.; Liu, Y. Design, synthesis and cytotoxic activities of novel 2,5-diketopiperazine derivatives. *Eur. J. Med. Chem.* **2016**, *4*, 500–509. [[CrossRef](#)]
37. Guo, X.; Ni, J.; Liang, Z.; Xue, J.; Fenech, M.F.; Wang, X. The molecular origins and pathophysiological consequences of micronuclei: New insights into an age-old problem. *Mutat. Res. Rev. Mutat. Res.* **2019**, *779*, 1–35. [[CrossRef](#)]
38. EFSA Scientific Committee (SC); More, S.J.; Bampidis, V.; Bragard, C.; Halldorsson, T.I.; Hernández-Jerez, A.F.; Hougaard Bennekou, S.; Koutsoumanis, K.; Lambré, C.; Machera, K.; et al. Guidance on aneugenicity assessment. *EFSA J.* **2021**, *19*, e06770. [[CrossRef](#)]
39. Li, Y.; Hecht, S.S. Metabolic Activation and DNA Interactions of Carcinogenic N-Nitrosamines to Which Humans Are Commonly Exposed. *Int. J. Mol. Sci.* **2022**, *23*, 4559. [[CrossRef](#)]
40. Ahmadian, E.; Eftekhari, A.; Kavetsky, T.; Khosroushahi, A.Y.; Turksoy, V.A.; Khalilov, R. Effects of quercetin loaded nanostructured lipid carriers on the paraquat-induced toxicity in human lymphocytes. *Pestic. Biochem. Physiol.* **2020**, *16*, 104586. [[CrossRef](#)]
41. Ozhan, G.; Alpertunga, B. Genotoxic activities of drug-nitrite interaction products. *Drug Chem. Toxicol.* **2003**, *26*, 295–308. [[CrossRef](#)] [[PubMed](#)]
42. Regulska, K.; Stanisz, B.; Lisiecki, P. Optimization of storage and manufacture conditions for imidapril hydrochloride in solid state as a way to reduce costs of antihypertensive therapy. *AAPS PharmSciTech* **2013**, *14*, 1199–1208. [[CrossRef](#)] [[PubMed](#)]

**Disclaimer/Publisher’s Note:** The statements, opinions and data contained in all publications are solely those of the individual author(s) and contributor(s) and not of MDPI and/or the editor(s). MDPI and/or the editor(s) disclaim responsibility for any injury to people or property resulting from any ideas, methods, instructions or products referred to in the content.